Optical signatures of electron correlations in the cuprates

D. van der Marel

In "Strong interactions in low dimensions"
series: Physics and Chemistry of Materials with Low-Dimensional Structures
Vol. 25
Dionys Baeriswyl (Editor), L. Degiorgi (Editor)
Kluwer (2005), VI, ISBN: 1-4020-1798-7

cond-mat/0301506.

Chapter 1

OPTICAL SIGNATURES OF ELECTRON CORRELATIONS IN THE CUPRATES

D. van der Marel
Laboratory of Solid State Physics
Materials Science Centre, University of Groningen
Nijenborgh 4, 9747 AG Groningen, The Netherlands
d.van.der.marel@phys.rug.nl

Abstract The f-sum rule is introduced and its applications to electronic and vibrational modes are discussed. A related integral over the intra-band part of $\sigma(\omega)$ which is also valid for correlated electrons, becomes just the kinetic energy if the only hopping os between nearest neighbor sites. A summary is given of additional sum rule expressions for the optical conductivity and the dielectric function, including expressions for the first and second moment of the optical conductivity, and a relation between the Coulomb energy and the energy loss function. It is shown from various examples, that the optical spectra of high T_c materials along the c-axis and in the ab-plane direction can be used to study the kinetic energy change due to the appearance of superconductivity. The results show, that the pairing mechanism is highly unconventional, and mostly associated with a lowering of kinetic energy parallel to the planes when pairs are formed.

Keywords: Optical conductivity, spectral weight, sum rules, reflectivity, dielectric function, inelastic scattering, energy loss function, inelastic electron scattering, Josephson plasmon, multi-layers, inter-layer tunneling, transverse optical plasmon, specific heat, pair correlation, kinetic energy, correlation energy, internal energy.

1. Macroscopic electromagnetic fields in matter

1.1 Introduction

The response of a system of electrons to an externally applied field is commonly indicated as the dielectric function, or alternatively as the

optical conductivity. The discussion in this chapter is devoted to induced currents and fields which are proportional to the external fields, the so-called linear response. The dielectric and the optical conductivity can be measured either using inelastic scattering of charged particles for which usually electrons are used, or by measuring the absorption of light, or the amplitude and/or phase of light reflected or transmitted by a sample. The two cases of fast particles and incident radiation involve different physics and will be discussed separately.

1.2 Reflection and refraction of electromagnetic waves

Optical spectroscopy measures the reflection and refraction of a beam of photons interacting with the solid. A rarely used alternative is the use of bolometric techniques to measure the absorption of photons directly. A variety of different experimental geometries can be used, depending on the type of sample under investigation, which can be a reflecting surface of a thick crystal, a free standing thin film, or a thin film supported by a substrate. Important factors influencing the type of analysis are also the orientation of the crystal or film surface, the angle of incidence of the ray of photons, and the polarization of the light. In most cases only the amplitude of the reflected or refracted light is measured, but sometimes the phase is measured, or the phase difference between two incident rays with different polarization as in ellipsometry. The task of relating the intensity and/or phase of the reflected or refracted light to the dielectric tensor inside the material boils down to solving the Maxwell equations at the vacuum/sample, sample/substrate, *etc.* interfaces. An example is the ratio of the reflection coefficients $(R_p/R_s)$and phase differences $(\eta_p - \eta_s)$ of light rays with p and s-polarization reflected on a crystal/vacuum interface at an angle of incidence θ. These quantities which are measured directly using ellipsometry

$$e^{i(\eta_p-\eta_s)}\sqrt{\frac{R_p}{R_s}} = \frac{\sin\theta\tan\theta - \sqrt{\epsilon - \sin^2\theta}}{\sin\theta\tan\theta + \sqrt{\epsilon - \sin^2\theta}} \tag{1.1}$$

The real and imaginary part of the dielectric constant can be calculated from such a measurement with the aid of Eq. 1.1. In contrast to a beam of charged particles, the electric field of a plane electromagnetic wave is transverse to the photon momentum. The dielectric tensor elements which can be measured in an optical experiment are therefore transverse to the direction of propagation of the electromagnetic wave. In a typical optical experiment the photon energy is below 6 eV. In vacuum the photon wave number used in optical experiments is therefore $0.0005\mathring{A}^{-1}$,

or smaller, which is at least three orders of magnitude below the Fermi momentum of electrons in a solid. For this reason it is usually said that optical spectroscopy measures the transverse dielectric constant or the optical conductivity at zero momentum. The optical conductivity tensor expresses the current response to an electrical field

$$\vec{j}(\vec{r},t) = \int d^3\vec{r}' \int dt' \sigma(\vec{r},\vec{r}',t-t')\vec{E}(\vec{r}',t') \tag{1.2}$$

From the Maxwell equations it can be shown that for polarization transverse to the propagation of an electromagnetic wave $d\vec{E}/dt = d\vec{D}/dt + 4\pi\vec{j}$. If the sample has translational invariance, the optical conductivity tensor has a diagonal representation in k-space. Due to the fact that the translational symmetries of a crystalline solid are restricted to a discrete space group, k is limited to the first Brillouin zone. Consequently, as shown by Hanke and Sham[1], the k-space representation of the dielectric tensor becomes a matrix in reciprocal space

$$\sigma(\vec{G},\omega)_{\vec{G},\vec{G}'} = \int d^2\vec{r} \int d^3\vec{r}' \int dt e^{i(\vec{q}+\vec{G})\cdot\vec{r}} e^{-i(\vec{q}+\vec{G}')\cdot\vec{r}'} e^{i\omega t} \sigma(\vec{r},\vec{r}',t) \tag{1.3}$$

The dependence of $\sigma(\vec{q},\omega)_{\vec{G},\vec{G}'}$ on the reciprocal lattice vectors $\vec{G}$, $\vec{G}'$ reflects, that the local fields can have strong variations in direction and magnitude on the length scale of a unit cell. Yet due to the long wavelength of the external light rays the Fresnel equations involve only $\vec{G} = \vec{G}' = 0$. Usually in texts on optical properties the only optical tensor elements considered have $\vec{G} = \vec{G}' = 0$, and in this chapter we will do the same.

Inside a solid the wavelength of the electromagnetic rays can be much shorter than that of a ray with the same frequency travelling in vacuum. Although in this chapter we will not encounter experiments where the finite momentum of the photon plays an important role, we should keep in mind that in principle the photon momentum is non-zero and can have a non-trivial effect on the optical spectra. In particular it may corrupt Kramers-Kronig relations, which is just one out of several reasons why spectroscopic ellipsometry should be favored.

1.3 Inelastic scattering of charged particles

When a fast charged particle, moving at a velocity $\vec{v}_e$, interacts weakly with a solid, it may recoil inelastically by transferring part of its momentum, $\hbar\vec{q}$ and its energy, $\hbar\omega$ to the solid. The fast electron behaves like a test charge of frequency $\omega = \vec{q}\cdot\vec{v}_e$, which corresponds to a dielectric displacement field, $D(\vec{r},t) = eq^{-2}\exp(i\vec{q}\cdot\vec{r} - i\omega t)$. The dielectric

displacement of the external charges may be characterized by a density fluctuation, which has no field component transverse to the wave. $D(\vec{r},t)$ is therefore a purely longitudinal field. In a solid mixing of transverse and longitudinal modes occurs whenever fields propagate in a direction which is not a high symmetry direction of the crystal. However, in the long wavelength limit the dielectric properties can be described by only three tensor elements which correspond to the three optical axes of the crystal. Since along these directions no mixing between longitudinal and transverse response occurs, we will consider the situation in this chapter where the fields and their propagation vector point along the optical axis. Inside a material the dielectric displacement is screened by the response of the matter particles, resulting in the screened field $E(\vec{r},t)$ inside the solid[1].

$$\vec{E}(\vec{r},t) = \int d^3\vec{r}' \int dt' \epsilon^{-1}(\vec{r},\vec{r}',t-t')\vec{D}(\vec{r}',t') \tag{1.4}$$

For the same reasons as for the optical conductivity the k-space representation of the dielectric tensor becomes a tensor in reciprocal space

$$\epsilon^{-1}(\vec{q}+\vec{G}',\vec{q}+\vec{G},\omega) = \int d^2\vec{r} \int d^3\vec{r}' \int dt e^{i(\vec{q}+\vec{G}')\cdot\vec{r}} e^{-i(\vec{q}+\vec{G})\cdot\vec{r}'} e^{i\omega t} \epsilon^{-1}(\vec{r},\vec{r}',t) \tag{1.5}$$

where $\vec{G}$ and $\vec{G}'$ denote reciprocal lattice vectors. The relation between the dielectric displacement and the electric field is

$$\vec{E}(\vec{q}+\vec{G}',\omega) = \sum_{\vec{G}} \epsilon^{-1}(\vec{q}+\vec{G}',\vec{q}+\vec{G},\omega)\vec{D}(\vec{q}+\vec{G},\omega) \tag{1.6}$$

The macroscopic dielectric constant, which measures the macroscopic response to a macroscopic perturbation, *i.e.* for vanishingly small $\vec{q}$, is given by[1]

$$\epsilon(\omega) = \lim_{q\to 0} \frac{1}{\epsilon^{-1}(\vec{q},\vec{q},\omega)} \tag{1.7}$$

where it is important, that in this expression first the matrix $\epsilon(\vec{q}+\vec{G}',\vec{q}+\vec{G},\omega)$ has to be inverted in reciprocal space, and in the next step the $(\vec{G}=0,\vec{G}'=0)$ matrix element is taken of the inverted matrix [1]. Energy loss spectroscopy using charged particles can be used to measure the dielectric response as a function of both frequency and momentum. This technique provides the longitudinal dielectric function, *i.e.* the response to a dielectric displacement field which is parallel to the transferred momentum $\vec{q}$. The probability per unit time that a fast electron transfers momentum $\vec{q}$ and energy $\hbar\omega$ to the electrons was

derived by Nozières and Pines[2, 3] for a fully translational invariant 'jellium' of interacting electrons

$$P(\vec{q},\omega) = \frac{8\pi e^2}{|q|^2}\mathrm{Im}\left\{\frac{-1}{\epsilon(\vec{q},\omega)}\right\} \tag{1.8}$$

where e is the elementary charge.

1.4 Relation between $\sigma(\omega)$ and $\epsilon(\omega)$

We close this introduction by remarking, that for electromagnetic fields propagating at a long wavelength the two responses, longitudinal and transverse, although different at any nonzero wave vector, are very closely related. We will take advantage of this fact when later in this chapter we extract the energy loss function for $q \approx 0$ from optical data. According to Maxwell's equations for $q \to 0$ the uniform current density is just the time derivative of the uniform dipole field, hence $4\pi j = i\omega(E - D)$. Consequently for $q \to 0$ the conductivity and the dielectric function are related in the following way

$$\epsilon(0,\omega) = 1 + \frac{4\pi i}{\omega}\sigma(0,\omega) \tag{1.9}$$

Throughout this chapter we will use this identity repeatedly.

2. Interaction of light with matter

2.1 The optical conductivity

Let us now turn to the discussion of the microscopic properties of the optical conductivity function. The full Hamiltonian describing the electrons and their interactions is

$$H = \sum_{k\sigma}\frac{\hbar^2k^2}{2m}c^\dagger_{k\sigma}c_{k\sigma} + \sum_G U_G\hat{\rho}_{-G} + \frac{1}{2}\sum_k V_k\hat{\rho}_{\vec{k}}\hat{\rho}_{-\vec{k}} \tag{1.10}$$

$$\hat{\rho}_{\vec{k}} = \sum_{p,\sigma}c^\dagger_{p,\sigma}c_{p+k,\sigma} \tag{1.11}$$

In this expression the symbol $c^\dagger_{p,\sigma}$ creates a plane wave of momentum $\hbar\vec{p}$ and spin-quantum number σ, U_G represents the potential landscape due to the crystal environment. The third term is a model electron-electron interaction Hamiltonian, representing all electron-phonon mediated and Coulomb interactions, where $\hat{\rho}_{\vec{k}}$ is the k'th Fourier component of the density operator. In addition to the direct Coulomb interaction, various other contributions may be relevant, such as direct exchange terms. As a result the spin- and momentum dependence of the total interaction can

have a more complex form than the above model Hamiltonian. Relevant for the subsequent discussion is only, that the interaction term commutes with the current operator. The quantum mechanical expression for the current operator is

$$\vec{j}_{\vec{q}} = \sum_{p,\sigma} \frac{e\hbar\vec{p}}{m} c^{\dagger}_{p-q/2,\sigma} c_{p+q/2,\sigma} \tag{1.12}$$

The current and density operators are symmetric in k-space, satisfying $\hat{\rho}^{\dagger}_k = \hat{\rho}_{-k}$ and $j^{\dagger}_k = j_{-k}$. In coordinate space the representations of the density and the current are

$$\hat{n}(\vec{r}) = \frac{1}{V} \sum_q e^{i\vec{q}\cdot\vec{r}} \hat{\rho}_{\vec{q}} \tag{1.13}$$

$$\vec{j}(\vec{r}) = \frac{e}{V} \sum_q e^{i\vec{q}\cdot\vec{r}} \vec{j}_{\vec{q}} \tag{1.14}$$

It is easy to verify, that together $\hat{n}(\vec{r})$ and $\vec{j}(\vec{r})$ satisfy the continuity equation $ie\hbar^{-1}[\hat{n}(\vec{r}), H] + \nabla \cdot \vec{j}(\vec{r}) = 0$.

Let us now consider a many-body system with eigen-states $|m\rangle$ and corresponding energies E_m. For such a system the microscopic expression for the optical conductivity has been explained by A.J. Millis in Chapter 6. The result for finite $\vec{q}$ was derived in 'The theory of quantum liquids' part I, by Nozières and Pines (equation 4.163). For brevity of notation we represent the matrix elements of the current operators as

$$j^{nm}_{\alpha,q} \equiv \langle n|j_{\alpha,q}|m\rangle \tag{1.15}$$

With the help of these matrix elements, and with the definition $\hbar\omega_{mn} = E_m - E_n$ the expression for the optical conductivity is

$$\sigma_{\alpha,\alpha}(\vec{q},\omega) = \frac{ie^2 N}{mV\omega} + \sum_{n,m\neq n} \frac{ie^{\beta(\Omega-E_n)}}{V\omega} \left[\frac{j^{nm}_{\alpha,q} j^{mn}_{\alpha,-q}}{\omega - \omega_{mn} + i\eta} - \frac{j^{nm}_{\alpha,-q} j^{mn}_{\alpha,q}}{\omega + \omega_{mn} + i\eta} \right] \tag{1.16}$$

Here N is the number of electrons, V the volume, m the electron mass, q_e the elementary charge, Ω is the thermodynamic potential, $\beta = 1/k_B T$ and η is an infinitesimally small positive number. In principle in the calculation of Eq. 1.16 terms may occur under the summation for which $\omega_{mn} = 0$. As ω_{mn} occurs in the denominator of this expression, these zeros should be cancelled exactly by zeros of the current matrix elements, which poses a special mathematical challenge.

In Eq. 1.16 $\sigma(\omega)$ is represented by two separate terms, a δ-function for $\omega = 0$ and a summation over excited many-body eigen-states. The

δ-function is a diamagnetic contribution of *all* electrons in the system, the presence of which is a consequence of the gauge invariant treatment of the optical conductivity, as explained by Millis in chapter 6. The presence of this term is at first glance rather confusing, since left by itself this δ-function would imply that all materials (including diamond) are ideal conductors! However, the second term has, besides a series of poles corresponding to the optical transitions, also a pole for $\omega = 0$, corresponding to a *negative* δ-function of $\mathrm{Re}\sigma(\omega)$. It turns out, that for all materials except ideal conductors this δ-function compensates exactly the first (diamagnetic) term of Eq. 1.16. This exact compensation is a consequence of the relation [6]

$$\text{For every } n\text{: } \sum_{m\neq n} \frac{j^{nm}_{\alpha,q} j^{mn}_{\alpha,-q}}{\omega_{mn}} = \frac{Ne^2}{2m} \tag{1.17}$$

Experimentally truly 'ideal' conductivity is only seen in superconductors. In ordinary conducting materials the diamagnetic term broadens to a Lorentzian peak due to elastic and/or inelastic scattering. The width of this peak is the inverse life-time of the charge carriers. Often in the theoretical literature the broadening is not important, and the Drude peak is counted to the Dirac-function in the origin. The infrared properties of superconductors are characterized by the presence of both a purely reactive diamagnetic response, and a regular dissipative conductivity [5]. The sum of these contributions counts the partial intra-band spectral weight which we discuss in section 2.4. With the help of Eq.1.17, the diamagnetic term of Eq. 1.16 can now be absorbed in the summation on the right-hand side

$$\sigma_{\alpha,\beta}(\vec{q},\omega) = \frac{i}{V} \sum_{n,m\neq n} \frac{e^{\beta(\Omega-E_n)}}{\omega_{mn}} \left\{ \frac{j^{nm}_{\alpha,q} j^{mn}_{\alpha,-q}}{\omega - \omega_{mn} + i\eta} + \frac{j^{nm}_{\alpha,-q} j^{mn}_{\alpha,q}}{\omega + \omega_{mn} + i\eta} \right\} \tag{1.18}$$

As explained in section 1.2, usually in optical experiments one assumes $q \to 0$ in the expressions for $\sigma(\omega)$. It is useful at this stage to introduce the generalized plasma frequencies $\Omega^2_{mn} = 8\pi e^{\beta(\Omega-E_n)} |j^{nm}_\alpha|^2 \omega^{-1}_{mn} V^{-1}$, with the help of which we obtain the following compact expression for the optical conductivity tensor

$$\sigma_{\alpha\alpha}(\omega) = \frac{i\omega}{4\pi} \sum_{n,m\neq n} \frac{\Omega^2_{mn}}{\omega(\omega + i\gamma_{mn}) - \omega^2_{mn}} \tag{1.19}$$

Although formally the parameter γ_{mn} is understood to be an infinitesimally small positive number, a natural modification of Eq.1.19 consists of limiting the summation to a set of oscillators representing the main

optical transitions and inserting a finite value for γ_{mn}, which in this case represents the inverse lifetime of the corresponding excited state (*e.g.* calculated using Fermi's Golden Rule). With this modification Eq.1.19 is one of the most commonly used phenomenological representations of the optical conductivity, generally known as the Drude-Lorentz expression.

2.2 The f-sum rule

The expressions Eqs. 1.16, 1.18, and 1.19 satisfy a famous sum rule. This is obtained by first showing with the help of Eq. 1.17, that for each n

$$\sum_{m,m\neq n} \Omega_{mn}^2 \equiv \frac{4\pi e^2 N}{mV} e^{\beta(\Omega - E_n)} \tag{1.20}$$

Second, as a result of Cauchy's theorem in Eq.1.19 the integral over all (positive and negative) frequencies of $\int \mathrm{Re}\sigma(\omega)$ equals $\sum_{mn} \Omega_{mn}^2/4$. To complete the derivation of the f-sum rule we also use that $\sum_n e^{\beta(\Omega - E_n)} = 1$, which follows from the definition of the thermodynamic potential. Then

$$\int_{-\infty}^{\infty} \mathrm{Re}\sigma(\omega) d\omega = \frac{\pi e^2 N}{mV} \tag{1.21}$$

is the f-sum rule, or Thomas-Reich-Kuhn rule. It is a cornerstone for optical studies of materials, since it relates the integrated optical conductivity directly to the density of charged objects, and the absolute value of their charge and mass. It reflects the fundamental property that also in strongly correlated matter the number of electrons is conserved. Note that the right-hand side of the f-sum rule is independent of the value of $\hbar$. Also the f-sum rule applies to bosons and fermions alike. Because $\mathrm{Re}\sigma(\omega)$=$\mathrm{Re}\sigma(-\omega)$ the sum rule is often presented as an integral of the conductivity over positive frequencies only. Superconductors present a special case, since $\mathrm{Re}\sigma(\omega)$ now has a δ function at $\omega = 0$: Only half of the spectral weight of this δ-function should be counted to the positive frequency side of the spectrum.

2.3 Spectral weight of electrons and optical phonons

The optical conductivity has contributions from both electrons and nuclei because each of these particles carries electrical charge. The integral over the optical conductivity can then be extended to the summation

over all species of particles in the solid with mass m_j, and charge q_j

$$\int_{-\infty}^{\infty} \mathrm{Re}\sigma(\omega)d\omega = \sum_j \frac{\pi q_j^2 N_j}{m_j V} \tag{1.22}$$

Because the mass of an electron is several orders of magnitude lower than the mass of a proton, in many cases the contribution of the nuclei to the f-sum rule is ignored in calculations of the integrated spectral weight of metals. However, important exceptions exist where the phonon contribution cannot be neglected, notably in the c-axis response of cuprate high T_c superconductors. Although Eq.1.22 is completely general, in practice it cannot be applied to experimental spectra directly. This is due to the fact that the contributions of all electrons and nuclei can only be obtained if the conductivity can be measured sufficiently accurately up to infinite frequencies. In practice one always uses a finite cut-off. Let us consider the example of an ionic insulator: If the integral is carried out for frequencies including all the vibrational modes, but does not include any of the inter-band transitions, then the degrees of freedom describing the motion of electrons relative to the ions is not counted. As a result the large number of electrons and nuclei which typically form the ions are not counted as separate entities. Effectively the ions behave as the only (composite) particles in such a case, and the right-hand side of Eq. 1.22 contains a summation over the ions in the solid. Application of Eq.1.22 provides the so-called transverse effective charge, which for ionic insulators with a large insulating gap corresponds rather closely to the actual charge of the ions. In the top panel of Fig. 1.1 this is illustrated with the infrared spectrum of MgO. Indeed the transverse effective charge obtained from the sum rule is 1.99, in good agreement with the formal charges of the Mg^{2+} and O^{2-} ions.

Because the mass of the ions is much higher than the free electron mass, the corresponding spectral weight integrated over the vibrational part of the spectrum is rather small. In a metal, even if optical phonons are present, usually the spectral weight at low frequencies is completely dominated by the electronic contributions due to the fact that the free electron mass is much smaller than the nuclear mass. A widely spread misconception is, that the screening of optical phonons in metals leads to a smaller oscillator strength than in ionic insulators. The opposite is true: Due to resonant coupling between vibrational modes and electronic oscillators, the optical phonons in an intermetallic compound often have much *more* spectral weight than optical phonons in insulators. This 'charged phonon' effect was formulated in an elegant way in 1977 by Rice, Lipari and Strässler[9]. They demonstrated, that under resonant conditions, due to electron-phonon coupling, vibrational

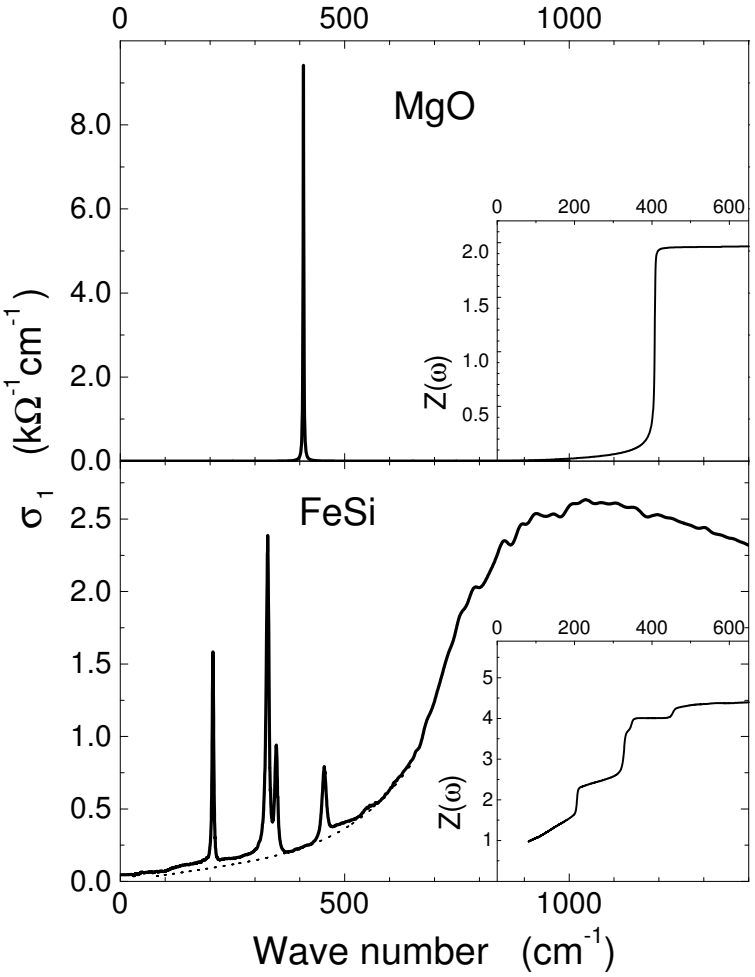

Figure 1.1. Optical conductivity of MgO (top panel) and FeSi at $T = 4$ K (bottom panel). In the insets the function $Z(\omega) = 8\mu(4\pi n_i e^2)^{-0.5}\left\{\int_0^\omega \sigma_{ph}(\omega')d\omega'\right\}^{0.5}$ is displayed. For FeSi the electronic background (dotted curve of the lower panel) was subtracted. For $\omega > 600\text{cm}^{-1}$ $Z(\omega)$ corresponds to transverse effective charge. Data from Ref. [7, 8].

modes borrow oscillator strength from electronic modes, which boosts the intensity of the vibrational modes in the optical conductivity spectra. This effect is now known to be common in many materials, for example in TCNQ-salts,blue bronze, IV-VI narrow-gap semiconductors, FeSi and related compounds, and the beta-phase of sodium vanadate [10, 11, 12, 13, 15, 8, 7, 14, 16]. In Figs. 1.1 and 1.2 the charged phonon effect is illustrated using the examples of FeSi, MnSi, CoSi and RuSi

[8, 7, 14], showing that the transverse charge is between 4 and 5. These compounds are not ionic insulators, because the TM and Si atoms have practically the same electro-negativities and electron affinities. Instead the large transverse charge of these compounds arises from the charged phonon effect predicted by Rice. The strong temperature dependence of the transverse charge of FeSi correlates with the gradual disappearance of the semiconductor gap as the temperature is raised from 4 to 300 K.

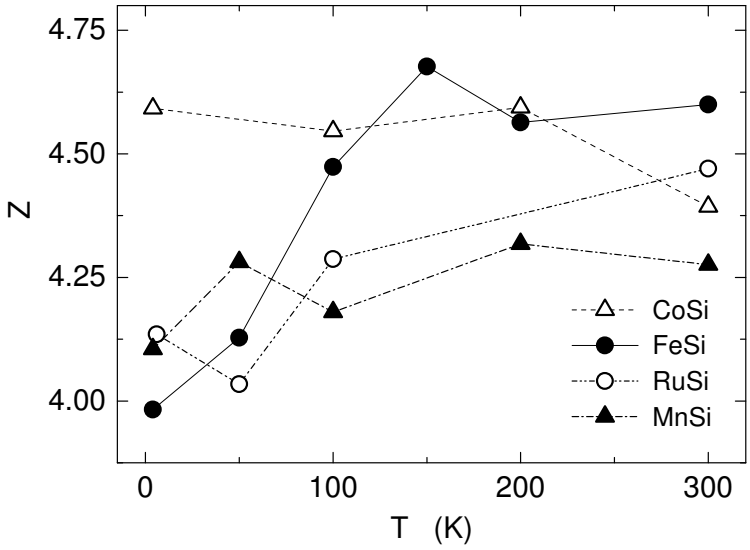

Figure 1.2. Temperature dependence of the transverse effective charge of Co-Si, Fe-Si, Ru-Si, and Mn-Si pairs, calculated from the oscillator strength of the optical phonons. Data from Refs. [7], [8] and [14].

2.4 Partial spectral weight of the intra-band transitions

Often there is a special interest in the spectral properties of the charge carriers. The electrons are subject to the periodic potential of the nuclei, resulting in an energy-momentum dispersion which differs from free electrons. Often one takes this dispersion relation as the starting point for models of interacting electrons. The Coulomb interaction and other (*e.g.* phonon mediated) interactions present the real theoretical challenge. The total Hamiltonian describing the electrons and their interactions is then

$$H = \sum_{k,\sigma} \epsilon_k c^\dagger_{k,\sigma} c_{k,\sigma} + \frac{1}{2} \sum_{kqp} V_k \sum_{\sigma\sigma'} c^\dagger_{p\sigma} c^\dagger_{q\sigma'} c_{q-k\sigma'} c_{p+k\sigma} \tag{1.23}$$

The current operator is in this case

$$\vec{j}_q = \frac{e}{2}\sum_{p,\sigma}\left(v_{p+q/2} - v_{-p+q/2}\right)c^{\dagger}_{p-q/2,\sigma}c_{p+q/2,\sigma} \tag{1.24}$$

where the $v_k \equiv \hbar^{-1}\partial\epsilon_k/\partial\vec{k}$ is the group velocity. The density operator commutes with the interaction part of the Hamiltonian. This has an interesting and very useful consequence, namely that a partial sum rule similar to the f-sum rule exists, which can be used to probe experimentally the kinetic energy term of the Hamiltonian. This partial sum rule for integration of the intra-band conductivity, $\sigma^L_{\alpha\alpha}(\omega)$, yields[17]

$$\int_{-\infty}^{\infty} d\omega \mathrm{Re}\sigma^L_{\alpha\alpha}(\omega)d\omega = \pi\frac{e^2}{V}\sum_{k,\sigma}\langle c^{\dagger}_{k,\sigma}c_{k,\sigma}\rangle\frac{1}{m_k} \tag{1.25}$$

$$\frac{1}{m_k} = \frac{1}{\hbar^2}\frac{\partial^2\epsilon(\vec{k})}{\partial k^2_\alpha} \tag{1.26}$$

Apparently the total spectral weight contained in the inter-band transitions, $\sigma^H_{\alpha\alpha}(\omega)$, is exactly

$$\int_{-\infty}^{\infty} d\omega \mathrm{Re}\sigma^H_{\alpha\alpha}(\omega) = \pi e^2\left(\frac{n}{m} - \frac{1}{V}\sum_k \frac{n_k}{m_k}\right) \tag{1.27}$$

In the limit where the interaction $V_k = 0$, the occupation function n_k in the above summation is a step-function at the Fermi momentum. In this case the summation over k becomes an integration over the Fermi volume with n_k set equal to 1. After applying Gauss's theorem we immediately obtain the well-known Fermi surface integral formula

$$\omega^2_{p,\alpha} = g\int_{S_F}\frac{e^2}{\hbar}v_\alpha(\vec{a})da_\alpha \tag{1.28}$$

where g is the spin degeneracy factor. In the literature two limiting cases are most frequently considered: (i) the free electron approximation, where $m_k = m_e$ is the free electron mass independent of the momentum of the electron, and (ii) the nearest neighbor tight-binding limit. In the latter case the dispersion is $\epsilon_k = -2t_x\cos k_x a_x - 2t_y\cos k_y a_y - 2t_z\cos k_z a_z$, with the effect that $1/m_k = -2t\hbar^{-2}a^2_\alpha\cos(k_\alpha a_\alpha)$, and

$$\sum_\alpha \frac{\hbar^2}{a^2_\alpha \pi e^2}\int_{-\omega_m}^{\omega_m}\mathrm{Re}\sigma_{\alpha\alpha}(\omega)d\omega = -\sum_{k,\sigma} n_k\epsilon_k = \langle -H_{kin}\rangle \tag{1.29}$$

where the integration should be carried out over all transitions within this band, *including* the δ-function at $\omega = 0$ in the superconducting state. The upper limit of the integration is formally represented by

the upper limit ω_m. In practice the cutoff cannot always be sharply defined, because usually there is some overlap between the region of transitions within the partially filled band and the transitions between different bands. Hence in the nearest neighbor tight-binding limit the f-sum provides the *kinetic energy* contribution, which depends both on the number of particles and the hopping parameter t[18]. This relation was used by Baeriswyl *et al.* to show, using exact results for one dimension, that the oscillator strength of optical absorption is strongly suppressed if the on-site electron-electron interactions (expressed by the Hubbard parameter U) are increased[19]. The same equation can also be applied to superconductors, examples will be discussed later in this chapter. In the case of a superconductor it is important to realize, that the integration on the left-hand side of Eq. 1.29 should also include the condensate δ-function at $\omega = 0$. As the optical conductivity can only be measured for $\omega > 0$, the spectral weight in the δ-function has to derived from a measurement of the imaginary part of $\sigma(\omega)$, taking advantage of the fact that the real and imaginary part of a δ-function conductivity are of the form

$$\sigma^{singular}(\omega) = \frac{2i\omega_{p,s}^2}{4\pi(\omega + i0^+)}$$

The plasma frequency of the condensate, $\omega_{p,s}$, is inversely proportional to the London penetration depth, $\lambda(T) = c/\omega_{p,s}(T)$ with c the velocity of light. In the literature[20, 21] the δ-function, conductivity integral for $\omega > 0$, and the kinetic energy are sometimes rearranged in the form

$$\frac{\omega_{p,s}^2}{8} = \frac{a^2\pi e^2}{2\hbar^2}\langle -H_{kin}\rangle - \int_{0^+}^{\omega_m} \mathrm{Re}\sigma(\omega)d\omega \tag{1.30}$$

Whenever the kinetic energy term on the right-hand side changes its value, this expression suggests a 'violation' of the f-sum rule, since the spectral weight in the δ-function now no longer compensates the change of spectral weight in the conductivity integration on the right-hand side. Of course there is no real violation, but part of the optical spectral weight is being swapped between the intra-band transitions and the inter-band transitions. Later in this chapter we will use the relation between kinetic energy as expressed in the original incarnation due to Maldague [18] (Eq. 1.29) to determine in detail the temperature dependence of the *ab*-plane kinetic energy of some of the high T_c superconductors.

It is easy to see, that for a small filling fraction of the band Eq. 1.29 is the same as the Galilean invariant result: The occupied electron states are now all located just above the bottom of the band, with an energy $-t$. Hence in leading orders of the filling fraction $-\langle\psi_g|H_t|\psi_g\rangle = Nt$. Identifying $a^2\hbar^{-2}t^{-1}$ as the effective mass m^* we recognize the familiar

f-sum rule, Eq.1.22, with the free electron mass replaced by the effective mass.

As the total spectral weight (intra-band plus inter-band) should satisfy the f-sum rule, the intra-band spectral weight is bounded from above, *i.e.* $0 \leq \sum_k n_k/m_k \leq n/m$. Near the top of the band the dynamical mass has the peculiar property that it is negative, $m_k < 0$, which in the present context adds a negative contribution to the intra-band spectral weight. On the other hand, the fact that $\mathrm{Re}\sigma(\omega)$ has to be larger than zero, implies that the equilibrium momentum distribution function n_k is subject to certain bounds: If for example n_k would preferentially occupy states near the top of the band, leaving the states at the bottom empty, the intra-band spectral weight would acquire an unphysical negative value. Apparently such momentum distribution functions cannot result from the interactions of Eq.1.23, regardless of the strength and k-dependence of those interactions.

2.5 Additional sum rules for $\sigma(\omega)$ and $1/\epsilon(\omega)$

Several other sum rule type expressions exist for the optical conductivity and for the dielectric constant. Here we give a summary. In the presence of a magnetic field an optical analogue of the Hall effect exists. The behavior is similar to the DC-limit, resulting in an off-diagonal component of the optical conductivity $\sigma_{xy}(\omega) = -\sigma_{yx}(\omega)$, where the z-axes is parallel to the magnetic field. The optical Hall angle is defined as

$$t_H(\omega) = \frac{\sigma_{xy}(\omega)}{\sigma_{xx}(\omega)} \tag{1.31}$$

The optical (σ_{xx}) and Hall conductivities(σ_{xy}) can be measured directly in optical transmission experiments [22, 23]. Drew and Coleman have shown[24] that this response function obeys the sum rule

$$\frac{2}{\pi}\int_0^\infty t_H(\omega)d\omega = \omega_H \tag{1.32}$$

where the Hall frequency ω_H is unaffected by interactions, and in the Galilean invariant case corresponds to the bare cyclotron frequency, $\omega_H = eB/m$.

A *first moment* sum rule of the optical conductivity is easily obtained for $T = 0$, by direct integration of Eq. 1.18, providing

$$\begin{array}{l} \int_0^\infty \omega\sigma_{\alpha,\alpha}(q,\omega)d\omega = \frac{2\pi}{\hbar V}\langle j_{\alpha,q} j_{\alpha,-q}\rangle = \\ = \frac{2\pi e^2\hbar}{m^2 V}\sum_{k,\sigma,\sigma'} k_\alpha^2 \langle c^\dagger_{k-q/2,\sigma} c_{k+q/2,\sigma'} c^\dagger_{k+q/2,\sigma'} c_{k-q/2,\sigma}\rangle \end{array} \tag{1.33}$$

In free space there is no scattering potential nor a periodic potential causing Umklapp scattering. Hence for electrons moving in free space

the right-hand side of Eq. 1.33 is exactly zero. This comes as no surprise: The integral on the left-hand side is also zero, since the optical conductivity of such a system has only a δ-function at $\omega = 0$ due to Galilean invariance. However, in the presence of Umklapp scattering the eigen-states of the electrons with energy-momentum dispersion ϵ_k are no longer the free electron states in the summation of Eq. 1.33. The true eigen-states are superpositions of plane waves. Vice versa the free electron states generated by the $c_k^\dagger$ operators of the above expression can be written as a superposition of the eigen-states of the periodic potential: $c_{k+G,\sigma}^\dagger = \sum_m \alpha_G^m(k) a_{k,m,\sigma}^\dagger$, where the latter operator generates the m'th eigen-state with momentum k in the first Brillouin zone. For brevity we introduce the notation $A_G^m = |\alpha_G^m(k)|^2$, and $\hat{n}_\sigma^j = a_{k,j,\sigma}^\dagger a_{k,j,\sigma}$. Expressed in terms of these band occupation number operators Eq. 1.33 is

$$\lim_{q\to 0} \int_0^\infty \omega \sigma_{\alpha,\alpha}(q,\omega) d\omega = \frac{2\pi e^2 \hbar}{m^2 V} \sum_{k,G} (k_\alpha + G_\alpha)^2 \sum_{j,m,\sigma} A_G^j A_G^m \langle \hat{n}_\sigma^j (1 - \hat{n}_\sigma^m) \rangle \tag{1.34}$$

The summation on the right-hand side strongly suggests an intimate relationship between the optical conductivity and the kinetic energy of the electrons. However, due to the fact that the expression on the right-hand side is rather difficult to calculate, the first moment of $\sigma(\omega)$ is of little practical importance. It's main purpose in the present context is to demonstrate the trend that an increase of the kinetic energy is accompanied by an increase of the first moment of the optical conductivity spectrum. This is consistent with the notion, that an increase of kinetic energy is accompanied by a blue-shift of the spectral weight.

For the energy-loss function a separate series of sum rule type equations can be derived[25, 26, 27]

$$\int_{-\infty}^{\infty} \mathrm{Im} \frac{-\omega}{\epsilon(\omega)} d\omega = \frac{4\pi^2 e^2 N}{mV} \tag{1.35}$$

which is similar to the f-sum rule for the optical conductivity, Eq. 1.22.

As a result of the fact that the real and imaginary part of the energy loss function are connected via Kramers-Kronig relations, the following relation exists

$$\int_{-\infty}^{\infty} \mathrm{Im} \frac{-1}{\omega \epsilon(\omega)} d\omega = \pi \tag{1.36}$$

This expression can in principle be used to calibrate the absolute intensity of an energy-loss spectrum, or to check the experimental equipment, since the right-hand side does not depend on any parameter of the material of which the spectrum is taken. We can use the relation between

$\epsilon(\omega)$ and $\sigma(\omega)$, Eq. 1.9, to express Eq. 1.36 as a function of $\sigma(\omega)$. Using Cauchy's theorem, it is quite easy to prove from Eq.1.36, that

$$\int_0^\infty \mathrm{Re}\frac{1}{\sigma(\omega) - i\lambda\omega}d\omega = \frac{\pi}{2\lambda} \tag{1.37}$$

Often the intra-band optical conductivity is analyzed in terms of a frequency dependent scattering rate $1/\tau(\omega) = (ne^2/m)\mathrm{Re}\{\sigma(\omega)^{-1}\}$, which follows directly from the experimental real and imaginary part of the optical conductivity. Taking the limit $\lambda \to 0$ in Eq.1.37, we observe that

$$\int_0^\infty \frac{1}{\tau(\omega)}d\omega = \lim_{\lambda\to 0}\frac{\pi}{2\lambda}\frac{ne^2}{m} = \infty \tag{1.38}$$

Hence ultraviolet divergency appears to be a burden of integral formulas of the frequency dependent scattering rate[28, 29, 30] which is hard to avoid.

In section 3.1 we will encounter a relation between the loss-function and the Coulomb energy stored in the electron fluid[26]

$$\int_0^\infty \mathrm{Im}\frac{-1}{\epsilon(\vec{k},\omega)}d\omega = \frac{4\pi^2 e^2}{\hbar|\vec{k}|^2}\langle\Psi_0|\hat{\rho}_k\hat{\rho}_{-k}|\Psi_0\rangle \tag{1.39}$$

This expression is limited to the ground state at $T = 0$, as was also the case for Eq. 1.33. The integrands on the left-hand side of Eq. 1.33 and Eq. 1.39 are *odd* functions of frequency. In contrast the f-sum rule, and the other expressions given in this subsection all involve integrals over an even function of frequency, which is the reason why the latter can be represented as integrals over all (positive and negative) frequencies. The fact that $\hbar$ occurs on the right-hand side of Eqs. 1.33 and 1.39 implies that these expressions are of a fundamental quantum mechanical nature, with no equivalent in classical physics.

Recently Turlakov and Leggett derived an expression for the *third* moment of the energy loss function, which in the limit of $k \to 0$ is a function of the Umklapp potential of Eq.1.11

$$\int_{-\infty}^\infty \mathrm{Im}\frac{-\omega^3}{\epsilon_{\alpha\alpha}(\omega)}d\omega = \frac{4\pi^2}{m^2}\left\langle -\sum_G G_\alpha^2 U_G\hat{\rho}_{-G}\right\rangle \tag{1.40}$$

The fact, that the right-hand side of Eq. 1.40 is finite implies, that for $\omega \to \infty$ the loss function of any substance must decay more rapidly than $\mathrm{Im}\{-\epsilon(\omega)^{-1}\} \propto \omega^{-4}$, and that the optical conductivity decays faster than $\mathrm{Re}\{\sigma(\omega)\} \propto \omega^{-3}$. This expression is potentially interesting for the measurement of changes in Umklapp potential, provided that experimental data can be collected up to sufficiently high photon energy, so that the left-hand side of the expression reaches its high frequency limit.

3. The internal energy of superconductors

A necessary condition for the existence of superconductivity is, that the free energy of the superconducting state is lower than that of the non-superconducting state. At sufficiently high temperature important contributions to the free energy are due to the entropy. These contributions depend strongly on the nature of the low energy excitations, first and foremost of all their nature be it fermionic, bosonic or of a more complex character due to electron correlation effects. At $T = 0$ the free energy and internal energy are equal, and are given by the quantum expectation value of the Hamiltonian, which can be separated into an interaction energy and a kinetic energy.

3.1 Interaction energy in BCS theory

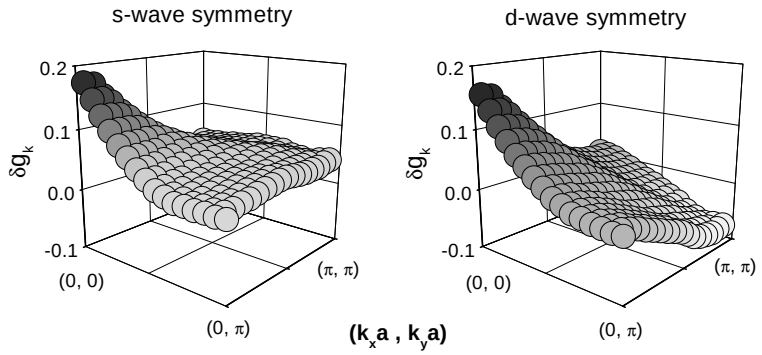

Figure 1.3. The k-space representation of the superconductivity induced change of pair correlation function for the s-wave (left panel) and d-wave symmetry (right panel). Parameters: $\Delta/W = 0.2$, $\omega_D/W = 0.2$. Doping level x = 0.25

We consider a system of electrons interacting via the interaction Hamiltonian given in Eq. 1.23. In the ground state of the system, the interaction energy, including the correlation energy beyond the Hartree-Fock approximation, is just the quantum expectation value of the second (interaction) term of 1.23. Here we are only interested in the difference in interaction energy between the normal and superconducting state.

$$E^s_{corr} - E^n_{corr} = \sum_k V_k \left(\langle \hat{\rho}_k \hat{\rho}_{-k} \rangle_s - \langle \hat{\rho}_k \hat{\rho}_{-k} \rangle_n \right) = \sum_k V_k \delta g_k \qquad (1.41)$$

In BCS theory the only terms of the interaction Hamiltonian which contribute to the pairing are the so-called reduced terms, *i.e.* those terms in the summation of Eq. 1.23 for which the center of mass momentum

$p+q=0$. The quantum mechanical expectation value of the correlation function is

$$\delta g_k = \sum_p (|u_{p+k}|^2 - \theta_{p+k})(\theta_p - |u_p|^2) + \sum_p u_{p+k} v_{p+k} u_p^* v_p^* \qquad (1.42)$$

The first term on the right-hand represents the change in exchange correlations, whereas the second term represents the particle-hole mixing which is characteristic for the BCS state. A quantity of special interest is the real space correlation function $\delta g(r,r') = \langle n(r)n(r')\rangle_s - \langle n(r)n(r')\rangle_n$. The Fourier transform of this correlation function is directly related to δg_k appearing in the expression of the interaction energy, Eq.1.41

$$\delta g_k = \frac{1}{V^2} \int d^3r \int d^3r' e^{ik(r-r')} \delta g(r,r') \qquad (1.43)$$

We see, that if the correlation function $\delta g(r,r')$ could be measured somehow, and the interaction V_k is known, than the interaction energy would follow directly from our knowledge of $\delta g(r,r')$:

$$E^s_{corr} - E^n_{corr} = \int d^3r \int d^3r' V(r-r') \delta g(r,r') \qquad (1.44)$$

In a conventional superconductor the quasi-particles of the normal state are also the fermions which become paired in the superconducting state. (Note, that now we are using the concept of Landau Fermi-liquid quasi-particles for the normal state. Later in this manuscript we will explore some consequences of *not* having a Fermi liquid in the normal state, where the quasi-particle concept will be abandoned.) Although the quasi-particle eigen-states of a conventional Fermi liquid have an amount of electron character different from zero, their effective masses, velocities and scattering rates are renormalized. The conventional point of view is, that pairing (enhancement of pair correlations) reduces the interaction energy of the electrons, by virtue of the fact that in the superconducting state the pair correlation function $g(r,r') = \langle \Psi | \hat{n}(r)\hat{n}(r') | \Psi \rangle$ increases at distances shorter than the superconducting coherence length ξ_0. If the interaction energy $V(r-r')$ is *attractive* for those distances, the interaction energy, Eq. 1.44, decreases in the superconducting state, and $V(r-r')$ represents a (or the) pairing mechanism. In Fig. 1.3 we show calculations of δg_k assuming a bandstructure of the form

$$\epsilon_k = \frac{W}{4} [\cos k_x a + \cos k_y a] - \mu \qquad (1.45)$$

while adopting an order parameter of the form

$$\Delta_k = \Delta_0 \Theta(|\epsilon_k - \mu| - \omega_D) \qquad (1.46)$$

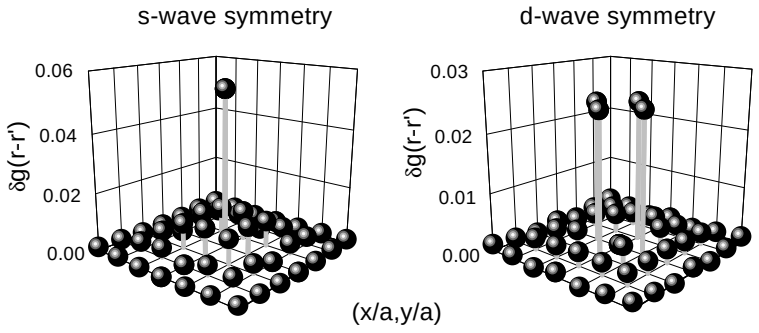

Figure 1.4. The coordinate space representation of the superconductivity induced change of pair correlation function for the s-wave (left panel) and d-wave symmetry (right panel). Parameters: $\Delta/W = 0.2$, $\omega_D/W = 0.2$. Doping level: x = 0.25

for s-wave symmetry, and

$$\Delta_k = \Delta_0 \left[\cos k_x a - \cos k_y a\right] \Theta(|\epsilon_k - \mu| - \omega_D) \tag{1.47}$$

for d-wave symmetry. The parameters used were $\Delta/W = 0.2$, $\omega_D/W = 0.2$, and $E_F/W = 0.43$ corresponding to x=0.25 hole doping counted from half filling of the band. The chemical potential in the superconducting state was calculated selfconsistently in order to keep the hole doping at the fixed value of x=0.25 [31, 32, 33, 34]. From Fig.1.3 we conclude that s-wave pairing symmetry requires a negative V_k regardless of the value of k, whereas the d-wave symmetry can be stabilized either assuming $V_k > 0$ for k in the (π, π) region, or $V_k < 0$ for k near the origin. Both types of symmetry are suppressed by having $V_k > 0$ at small momentum, such as the Coulomb interaction.

In Fig. 1.4 we display the correlation function in coordinate space representation. This graph demonstrates, that d-wave pairing is stabilized by a nearest-neighbor attractive interaction potential. An on-site *repulsion* has no influence on the pairing energy, since the pair correlation function has zero amplitude for $r - r' = 0$. On the other hand, for s-wave pairing the 'best' interaction is an on-site attractive potential, since the s-wave $\delta g(r, r')$ reaches it's maximum value at $r - r' = 0$.

3.2 Experimental measurements of the Coulomb interaction energy

In a series of papers Leggett has discussed the change of Coulomb correlation energy for a system which becomes superconducting[35], and has argued, that this energy would actually decrease in the superconducting state. Experimentally the changes of Coulomb energy can be

measured directly in the sector of k-space of vanishing k. The best, and most stable, experimental technique is to measure the dielectric function using spectroscopic ellipsometry, and to follow the changes as a function of temperature carefully as a function of temperature. Because the cuprates are strongly anisotropic materials, it is crucial to measure both the in-plane and out-of-plane pseudo-dielectric functions, from which the full dielectric tensor elements along the optical axes of the crystal then have to be calculated. We followed this procedure for a number of different high T_c cuprates, indicating that the Coulomb energy in the superconducting state *in*creases for k=0. However, for $k \neq 0$ this need no longer be the case. Summarizing the situation[36]: the Coulomb interaction energy increases in the superconducting state for small k. This implies, that the lowering of internal energy in the superconducting state must be caused either by other sectors of k-space (in particular at around the (π, π) point, see Fig. 1.3!), or by a lowering of the kinetic energy in the superconducting state. The latter is only possible in a non Fermi liquid scenario of the normal state.

3.3 Kinetic energy in BCS theory

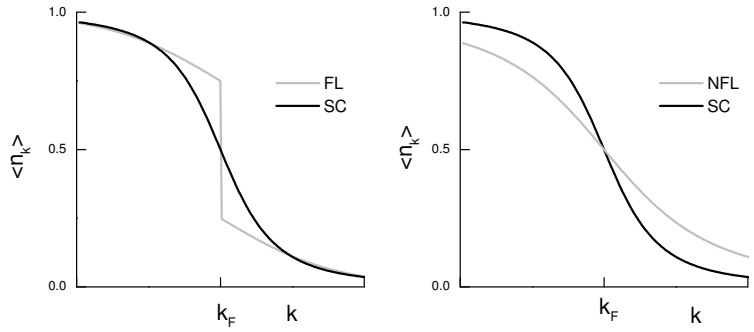

Figure 1.5. Occupation function as a function of momentum in the normal (dash) and the superconducting (solid) state for Fermi liquid (left panel) and an example of a broad distribution function, not corresponding to a Fermi liquid (right panel).

In BCS theory the lowering of the pair-interaction energy is partly compensated by a change of kinetic energy of opposite sign. This can be understood qualitatively in the following way: The correlated motion in pairs causes a localization of the relative coordinates of electrons, thereby increasing the relative momentum and the kinetic energy of the electrons. Another way to see this, is that in the superconducting state the step of n_k at the Fermi momentum is smoothed, as indicated in the left panel of Fig. 1.5, causing E_{kin} to become larger[37].

A pedagogical example where the kinetic energy of a pair is higher in the superconducting state, is provided by the negative U Hubbard model[38]: Without interactions, the kinetic energy is provided by the expression

$$E_{kin} = -t \sum_{<i,j>,\sigma} \langle \Psi | c^{\dagger}_{i\sigma} c_{j\sigma} + H.c. | \Psi \rangle \tag{1.48}$$

Let us consider a 2D square lattice. If the band contains two electrons, the kinetic energy of each electron is $-2t$, the bottom of the band, hence $E_{kin} = -4t$. (In a tight-binding picture the reference energy is the center of the band irrespective of E_F, causing E_{kin} to be always negative). Let us now consider the kinetic energy of a pair in the extreme pairing limit, *i.e.* $U \gg t$, causing both electrons to occupy the same site, with an interaction energy $-U$. The occupation function n_k in this case becomes

$$n_k \approx \frac{1}{N_k} \frac{t}{U} \frac{1}{(1 + 4\epsilon_k/U)^2} \tag{1.49}$$

This implies that the kinetic energy approaches $E_{kin} \rightarrow -8t^2/U$. Hence the kinetic energy increases from $E^n_{kin} = -4t$ to $E^s_{kin} = -\frac{8t^2}{U}$ when the local pairs are formed. The paired electrons behave like bosons of charge $2e$. A second order perturbation calculation yields an effective boson hopping parameter[39] $t' = t^2/U$. In experiments probing the charge dynamics, this hopping parameter determines the inertia of the charges in an accelerating field. As a result the plasma frequency of such a model would be

$$\omega^2_{p,s} = 4\pi \frac{n}{2} (2e)^2 \frac{a^2 t^2}{\hbar^2 U} \tag{1.50}$$

whereas if these pair correlations are muted

$$\omega^2_{p,n} = 4\pi n e^2 \frac{a^2 t}{\hbar^2} \tag{1.51}$$

Because the plasma frequency is just the low frequency spectral weight associated with the charge carriers, this demonstrates, that for conventional pairs (*i.e.* those which are formed due to interaction energy lowering) the expected trend is, that in the superconducting state the spectral weight *de*creases. Note, that this argument can only demonstrate the direction in which the plasma frequency changes when the pair correlations become reduced, but it does not correctly provide the quantitative size of the change, since the strong coupling regime of Eq. 1.50 implies the presence of a finite fraction of uncondensed 'preformed' pairs in the normal state. The same effect exists in the limit of weak pairing correlations. In Ref. [40] (Eq. 29, ignoring particle-hole asymmetric terms)

the following expression was derived for the plasma resonance

$$\omega_{p,s}^2 = \frac{4\pi e^2}{V} \sum_k \frac{\Delta_k^2}{\hbar^2 E_k^3} \left[\frac{\partial \epsilon_k}{\partial k}\right]^2 \tag{1.52}$$

where V is the volume of the system, and $E_k^2 = \epsilon_k^2 + |\Delta_k|^2$. Integrating in parts, using that $\Delta_k^2 E_k^{-3} \partial_k \epsilon_k = \partial_k \left(\epsilon_k / E_k\right)$, and that $\partial_k \epsilon_k = 0$ at the zone-boundary, we obtain

$$\omega_{p,s}^2 = \frac{4\pi e^2}{V} \sum_k \frac{n_k}{m_k} \tag{1.53}$$

where $m_k^{-1} = \hbar^{-2} \partial^2 \epsilon_k / \partial k^2$, and $n_k = 1 - \epsilon_k / E_k$. For a monotonous band dispersion the plasma frequency of the superconductor is always *smaller* than that of the unpaired system: Because the sign of the band-mass changes from positive near the bottom of the band to negative near the top, the effect of the broadened occupation factors n_k is to give a slightly smaller average over m_k^{-1}, hence ω_p^2 is smaller. Note that the mass of free electrons does not depend on momentum, hence in free space ω_p^2 is unaffected by the pairing.

To obtain an estimate of the order of magnitude of the change of spectral weight, we consider a square band of width W with a Fermi energy $E_F = N_e/(2W)$, where N_e is the number of electrons per unit cell. To simplify matters we assume that $1/m_k$ varies linearly as a function of band energy:$1/m(\epsilon) = (W - 2E_F - 2\epsilon)/(Wm_0)$. We consider the limit where $\Delta << W, E_F$. Let us assume that the bandwidth $\sim$ 1 eV, and $\Delta \sim$ 14 meV corresponding to T_c =90 K. The reduction of the spectral weight is then 0.28 %. If we assume that the bandwidth is 0.1 eV, the spectral weight reduction would typically be 11.4 %.

3.4 Kinetic energy driven superconductivity

If the state above T_c is *not* a Fermi liquid, the situation could be reversed. The right-hand panel of Fig.1.5 represents a state very different from a Fermi liquid, and in fact looks similar to a gapped state. Indeed even for the 1D Luttinger liquid $n(k)$ has an infinite slope at k_F. If indeed the normal state would have a broad momentum distribution like the one indicated, the total kinetic energy becomes lower once pairs are formed, provided that the slope of $n(k)$ at k_F is steeper in the superconducting state. This is not necessarily in contradiction with the virial theorem, even though ultimately all relevant interactions (including electron-phonon interactions) are derived from the Coulomb interaction: The superconducting correlations involve the low energy

scale quasi-particle excitations and their interactions. These *effective* interactions usually have characteristics quite different from the original Coulomb interaction, resulting in $E_c/E_{kin} \neq -2$ for the low energy quasi-particles. Various models have been recently proposed involving pairing due to a *reduction* of kinetic energy. In strongly anisotropic materials such as the cuprates, two possible types of kinetic energy should be distinguished: Perpendicular to the planes[41, 42] (along the c-direction) and along the planar directions[43, 44, 45, 46, 47, 48, 49, 50, 51].

4. Experimental studies of superconductivity induced spectral weight transfer

4.1 Josephson plasmons and c-axis kinetic energy

C-axis kinetic energy driven superconductivity has been proposed within the context of inter-layer tunneling, and has been extensively discussed in a large number of papers[43, 44, 41, 52, 42, 21, 53, 54, 55, 56, 57, 20, 58, 59, 60, 61, 62, 63, 64]. One of the main reasons to suspect that superconductivity was c-axis kinetic driven, was the observation of "incoherent" c-axis transport of quasi-particles in the normal state[65] and, rather surprisingly, *also* in the superconducting state[66, 67, 68], thus providing a channel for kinetic energy lowering for charge carriers as soon as pairing sets in. As discussed in section 2.4 a very useful tool in the discussion of kinetic energy is the low frequency spectral weight associated with the charge carriers. In infrared spectra this spectral weight is contained within a the 'Drude' conductivity peak centered at $\omega = 0$. Within the context of the tight-binding model a simple relation exists between the kinetic energy per site, with volume per site V_u, and the low frequency spectral weight[18, 19]

$$E_{kin} = \frac{\hbar^2 V_u}{4\pi e^2 a^2}\omega_p^2 \tag{1.54}$$

Here the plasma frequency, ω_p, is used to quantify the low frequency spectral weight:

$$\frac{\omega_{p,s}^2}{8} + \int_{0^+}^{\omega_m} \mathrm{Re}\sigma(\omega)d\omega = \frac{1}{8}\omega_p^2 \tag{1.55}$$

where the integration should be carried out over all transitions within the band, *including* the δ-function at $\omega = 0$ in the superconducting state. The $\delta(\omega)$ peak in $\mathrm{Re}\sigma(\omega)$ is of course not visible in the spectra directly. However the presence of the superfluid is manifested prominently in the London term of $\mathrm{Re}\epsilon(\omega)$ (proportional to $\mathrm{Im}\sigma(\omega)$): $\epsilon_L(\omega) = -\omega_{p,s}^2\omega^{-2}$. In $La_{2-x}Sr_xCuO_4$ the London term is manifested in a spectacular way

as a prominent plasma resonance perpendicular to the superconducting planes[69]. This is commonly used to determine the superfluid spectral weight, $\omega_{p,s}^2$, from the experimental spectra. Apart from universal prefactors, the amount of spectral weight of the $\delta(\omega)$ conductivity peak corresponds to the Josephson coupling energy, which in turn is the inter-layer *pair*hopping amplitude. It therefore provides an upper limit to the change of kinetic energy between the normal and superconducting state [41, 52], because the spectral weight transferred from higher frequencies to the $\delta(\omega)$-peak cannot exceed this amount. This allowed a simple experimental way to test the idea of c-axis kinetic energy driven superconductivity by comparing the experimentally measured values of the condensation energy (E_{cond}) and E_J. The inter-layer tunneling hypothesis required, that $E_J \approx E_{cond}$. In the spring of 1996 the first experimental results were presented[53] for Tl2201 (Tc=80 K), showing that E_J was at least two orders of magnitude too small to account for the condensation energy. Later measurements of λ_c[57] (approximately 17 μm) and the Josephson plasma resonance (JPR)[56] at 28 cm^{-1}, allowed a definite determination of the Josephson coupling energy of this compound, indicating that $E_J \approx 0.3\mu$eV in Tl2201 with $T_c = 80$ K (see Fig. 1.7). This is a factor 400 lower than $E_{cond} \approx 100\mu$eV per copper, based either on c_V experimental data[70], or on the formula $E_{cond} = 0.5N(0)\Delta^2$ with $N(0) = 1eV^{-1}$ per copper, and $\Delta \simeq 15meV$. In Fig. 1.8 the change in c-axis kinetic energy and the Josephson coupling energies are compared to the condensation energy for a large number of high T_c cuprates. For most materials we see that $E_J < E_{cond}$, sometimes differing by several orders of magnitude.

These arguments falsifying the inter-layer tunneling mechanism have been questioned[21], arguing that a large part of the specific heat of Tl2201 is due to 3D fluctuations, and that these fluctuations should be subtracted when the condensation energy is calculated. However, it was recently shown[71] that due to thermodynamical constraints the fluctuation correction can not exceed a factor 2.5 in the case of Tl2201 (as compared to a factor 40 in Ref. [21]). Hence the discrepancy between the Josephson coupling energy and the condensation energy of Tl2201 is still two orders of magnitude.

However, as stressed above, E_J provides only an *upper limit* for ΔE_{kin}. A c-axis kinetic energy change *smaller* than E_J is obtained if we take into account the fact that a substantial part of $\delta(\omega)$-function is just the spectral weight removed from the sub-gap region of the optical conductivity. Usually it is believed that in fact the latter is the *only* source of intensity of spectral weight for the δ-function, known as the (phenomenological) Glover-Tinkham-Ferell[72] sum rule. According to the arguments given

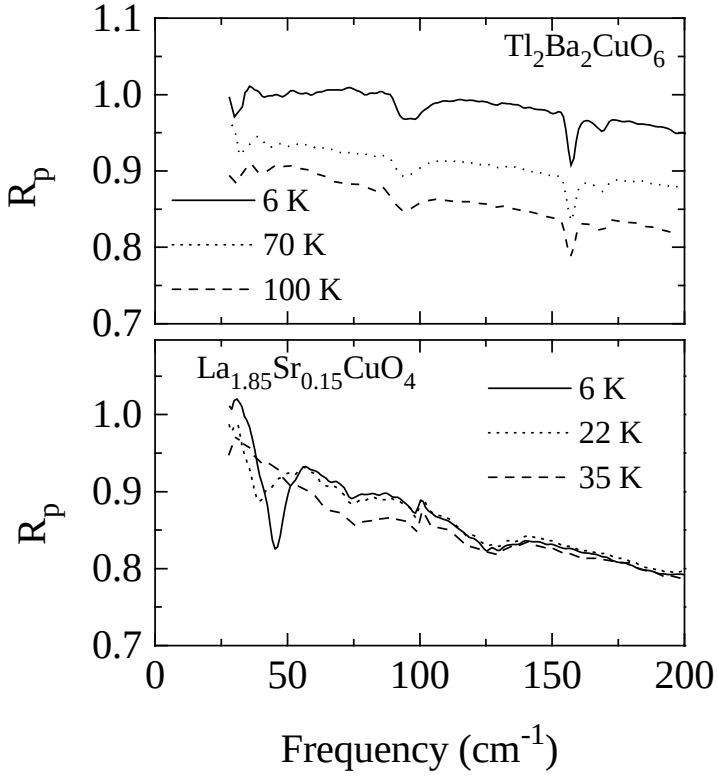

Figure 1.6. Grazing reflectivity of a $Tl_2Ba_2CuO_6$ thin film (upper panel) and $La_{1.85}Sr_{0.15}CuO_4$ single crystal (lower panel) measured with the polarization of the incident light tilted at an angle of 80° relative to the copper-oxygen planes. For LSCO the Josephson plasma resonance can be clearly seen at 40 cm^{-1}. For Tl2212 no the Josephson plasma resonance is observed, indicating that it is located below the lower limit of 30 cm^{-1} of the spectrometer. This implies that the Josephson coupling energy in this compound is at least two orders of magnitude lower than required by the inter-layer tunneling hypothesis. Data from Ref. [54]

in section 3.4 we may conclude that $E_{kin,s} = E_{kin,n}$ when we observe, that *all* spectral weight origins from the far-infrared gap region in agreement with the Glover-Tinkham-Ferrell sum rule. If, on the other hand, superconductivity is accompanied by a lowering of c-axis kinetic energy, part of $\omega_{p,s}^2$ originates from the higher frequency region of inter-band transitions, which begins at typically 2 eV. In other words, we may say that $\omega_{p,s}^2$ is an upper limit to the kinetic energy change

$$0 < E_{kin,n} - E_{kin,s} < \frac{\hbar^2 V_u}{4\pi e^2 a^2} \omega_{p,s}^2 \tag{1.56}$$

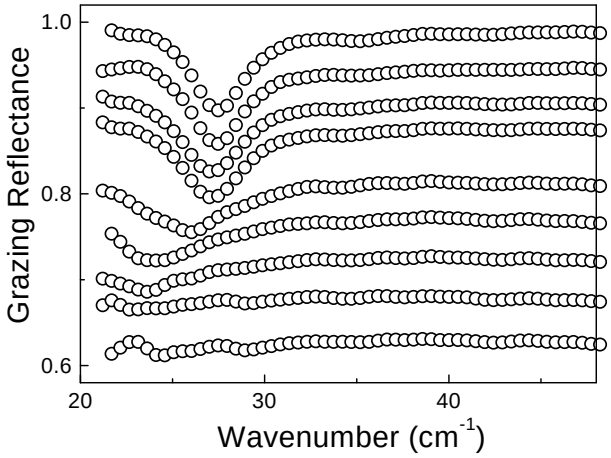

Figure 1.7. P-polarized reflectivity at 80^o angle of incidence of $Tl_2Ba_2CuO_6$. From top to bottom: 4K, 10 K, 20 K, 30 K, 40 K, 50 K, 60 K, 75 K, and 90 K. The curves have been given incremental 3 percent vertical offsets for clarity. Data from Ref. [56]

A direct determination of $E_{kin,s} - E_{kin,n}$ is obtained by measuring experimentally the amount of spectral weight transferred to the $\delta(\omega)$ peak due to the passage from the normal to the superconducting state, as was done by Basov *et al.*[20, 60]. These data indicated that for underdoped materials about 60% comes from the sub-gap region in the far infrared, while about 40% originates from frequencies much higher than the gap, whereas for optimally doped cuprates at least 90% originates from the gap-region, while less than 10% comes from higher energy. Experimental artifacts caused by a very small amount of mixing of ab-plane reflectivity into the c-axis reflectivity curves may have resulted in an overestimation of the spectral weight originating from high energies[60], in particular those samples where the electronic $\sigma_c(\omega)$ is very low due to the 2-dimensionality. Optimally doped YBCO is probably less prone to systematic errors due to leakage of R_{ab} into the c-axis reflectivity, since $\sigma_c(\omega)$ of this material is among the largest in the cuprate family. The larger $\sigma_c(\omega)$ causes the c-axis reflectivity to be much larger at all frequencies, thereby reducing the effect of spurious mixing of *ab*-plane reflectivity in the optical spectra on the Kramers-Kronig analyzes.

In summary $\Delta E_{kin,c} < 0.1 E_J$ in most cases. For several of the single-layer cuprates it has become clear now, that ΔE_{kin} significantly undershoots the condensation energy, sometimes by two orders of magnitude or worse, as indicated in Fig. 1.8.

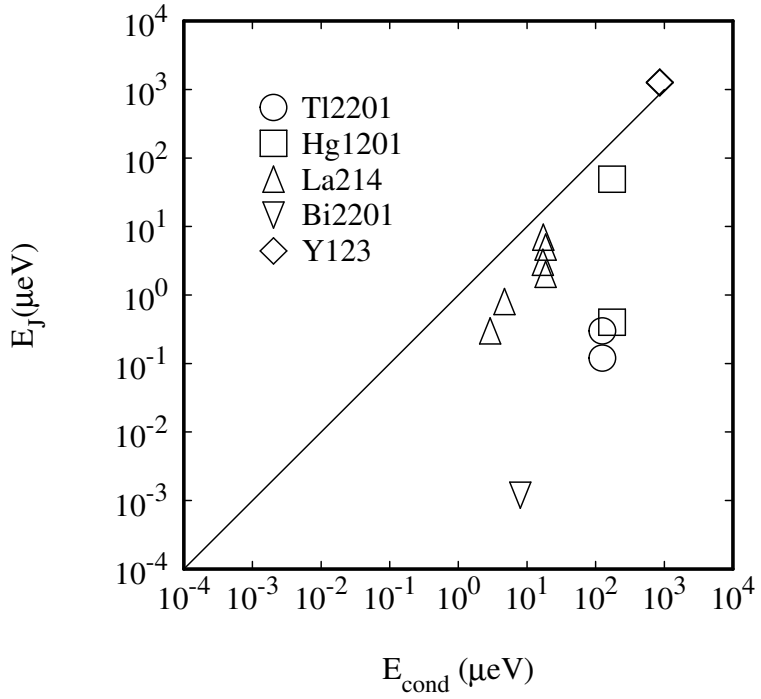

Figure 1.8. Intrinsic Josephson coupling energy [20, 55, 56, 57, 58, 59, 66, 69, 75] versus condensation energy[70, 76]

4.2 Josephson plasmons in multi-layered cuprates

This situation may be different for the bi-layer compounds. In these materials in principle the coupling within the bi-layer may provide an additional source of frustrated inter-layer kinetic energy, which can in principle be released when the material enters the superconductng state. This can in principle be monitored with infrared spectroscopy, because quite generally a stack of Josephson coupled layers with two different types of weak links alternating (in the present context corresponding to inter-bilayer and intra-bilayer) should exhibit three Josephson collective modes instead of one: Two of those modes are longitudinal Josephson plasma resonances, which show up as peaks in the energy loss function $\mathrm{Im}(-1/\epsilon(\omega))$. In between these two longitudinal resonances one expects a transverse optical plasma resonance, which is revealed by a peak in $\mathrm{Re}\sigma(\omega)$. In essence the extra two modes are out-of-phase oscillations of the two types of junctions. This has been predicted in Ref. [77] for the case of a multi-layer of Josephson coupled 2D superconducting lay-

ers. Further detailed calculations for the bi-layer case were presented in Refs. [78, 79]. The existence of *two* longitudinal modes and *one* associated transverse plasmon mode at finite frequencies has been confirmed experimentally for the $SmLa_{0.8}Sr_{0.2}CuO_{4-\delta}$ in a series of papers [80, 81, 82, 83, 84] (see Fig. 1.9).

The c-axis optical conductivity of YBCO is one order of magnitude larger than for LSCO near optimal doping. As a result the relative importance of the optical phonons in the spectra is diminished. In the case of optimally doped YBCO, the experiments indicate no significant transfer of spectral weight from high frequencies associated with the onset of superconductivity. C-axis reflectivity data[75] of optimally doped YBCO are shown in Figs.1.10. Above T_c the optical conductivity is weakly frequency dependent, and does not resemble a Drude peak. Below T_c the conductivity is depleted for frequencies below 500 cm^{-1}, reminiscent of the opening of a large gap, but not an s-wave gap, since a relatively large conductivity remains in this range.

There is a slight overshoot of the optical conductivity in the region between 500 and 700 cm^{-1}, due to the fact that the normal state and superconducting state curves cross at 600 cm^{-1}. In the case of the bi-layer cuprates this could be explained as a result of the presence of two superconducting layers per unit cell, resulting in the 'transverse optical' plasma mode mentioned above[62, 63, 64, 73, 74, 75].

For the f-sum rule the presence of this extra mode makes no difference. The extra spectral weight in the superconducting state associated with this mode has in principle the same origin as the spectral weight in the zero-frequency δ-function. In a conventional picture the source would be the spectral weight, removed due to a depletion of $\sigma_c(\omega)$ in the gap-region. The implementation of the sum rule relevant for this case then states that the relative spectral weight function

$$\frac{\Delta A(\omega)}{\omega_{p,s}^2} = \frac{8}{\omega_{p,s}^2} \int_{0^+}^{\omega} \left(\sigma_n(\omega') - \sigma_s(\omega')\right) d\omega' \tag{1.57}$$

overshoots the 100 % line close to the 'second plasma' mode, and saturates at 100 % for frequencies far above this mode. This is indeed observed in Fig. 1.10.

Additional studies of the bi-layer (and tri-layer) materials have provided confirmation of the transverse optical plasmon in these materials. In spite of its high frequency, making the assignment to the Josephson effect rather dubious, nevertheless the transverse optical mode either makes its first appearance below T_c, or gains in sharpness and intensity at the temperature where pairs are being formed (which for under-doped cuprates begins already above T_c). Also in at least a number of cases

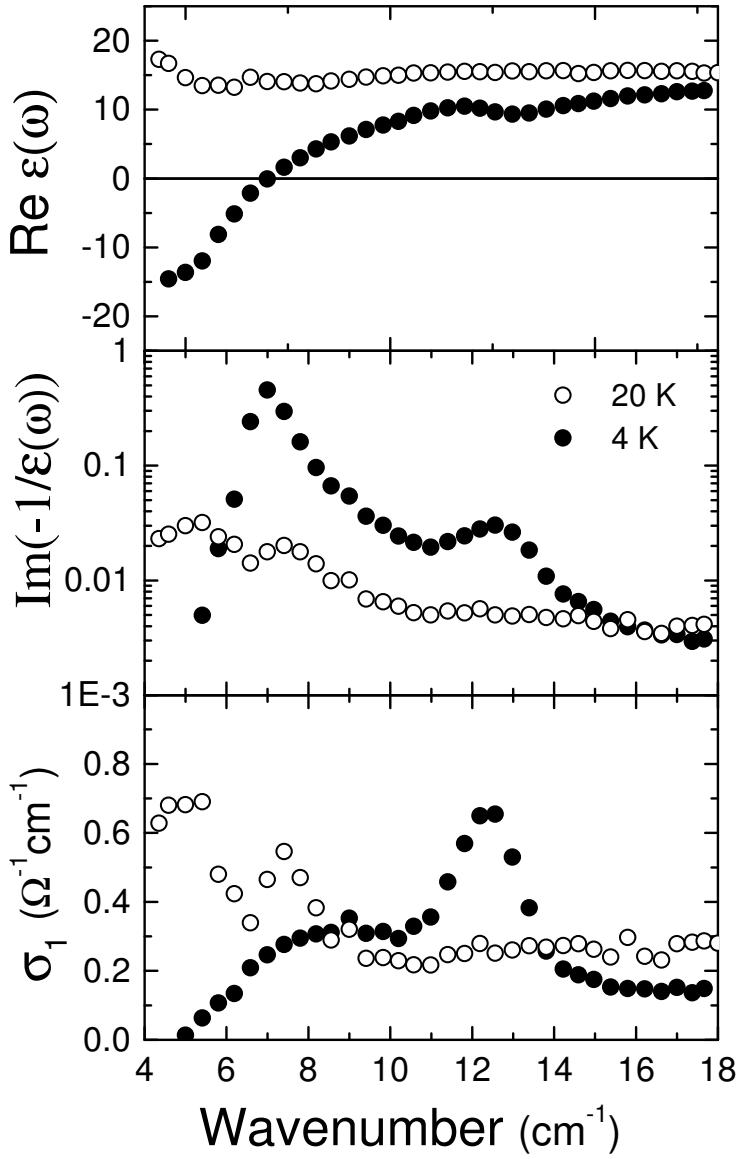

Figure 1.9. (a) Real part of the c-axis dielectric function of $SmLa_{0.8}Sr_{0.2}CuO_{4-\delta}$ for 4 K (closed symbols), and 20 K (open symbols) (b) The c-axis loss function, $\mathrm{Im}\epsilon(\omega)^{-1}$. (c) Real part of the c-axis optical conductivity. Data from Ref. [83, 85].

the spectral weight of the 'transverse optical' plasmon observed below T_c appears to originate not from the spectral weight removed from the gap region, but from much higher energies[60, 61, 62, 63, 64]. The impli-

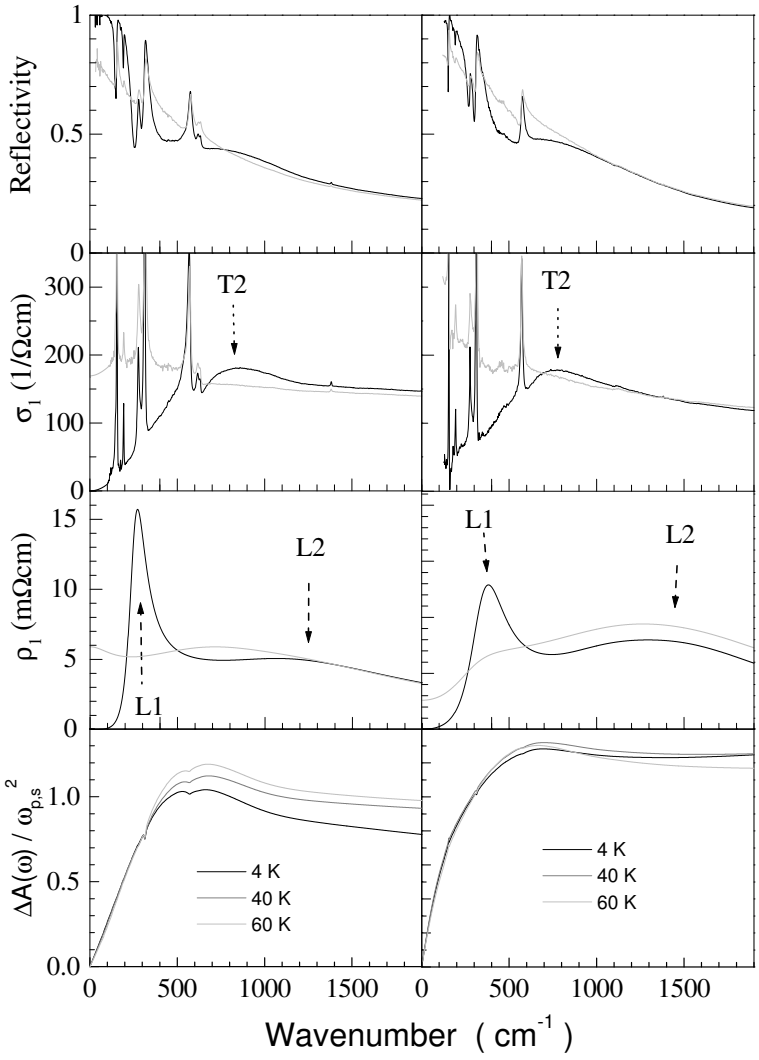

Figure 1.10. C-axis optical spectra of optimally doped (x=6.93) and over-doped (x=7.0) $YBa_2Cu_3O_{7-x}$. From top to bottom: reflectivity, optical conductivity, dynamical impedance and relative spectral weight (Eq. 1.57). The dynamical impedance, $\rho_1(\omega)$=Re$4\pi/\omega\epsilon(\omega)$ is proportional to the energy loss function weighted by a factor $1/\omega$. The optical phonons have been subtracted from the loss-functions for clarity. The data are from Ref. [75, 86]

cation of this may be, that a non-negligible fraction of frustrated c-axis kinetic energy is released when these materials become superconducting. This seems to be particularly relevant for the strong intra-bilayer (or tri-layer) coupling of Bi2212, Bi2223 and Y123.

4.3 Kinetic energy parallel to the planes

In-plane kinetic energy driven superconductivity has been proposed by a number of researchers: Hirsch[43, 44, 87] discussed this possibility as a consequence of particle-hole asymmetry. It has also been discussed within the context of holes moving in an anti-ferromagnetic background [88, 89, 90, 91, 92, 93]. More recently the possibility of a *reduction* of kinetic energy associated with pair hopping between stripes has been suggested[47, 51], and an in-plane pair delocalization mechanism have been proposed in the context of the resonating valence band model[49, 50].

A major issue is the question how to measure this. The logical approach would be to measure again $\sigma(\omega, T)$ using the combination of reflectivity and Kramers-Kronig analysis, and then compare the spectral weight function in the superconducting state to the same above T_c. There are several weak points to this type of analysis. In the first place there is the problem of sensitivity and progression of experimental errors: Let us assume, that the change of kinetic energy is of order 0.1 meV per Cu atom (this is approximately the condensation energy of the optimally doped single layer cuprate Tl2201, with $T_c = 85$ K.). For an inter-layer spacing of 1.2 nm, this corresponds to a spectral weight change $\Delta(\nu_p^2) = 10^5$ cm^{-2}. As the total spectral weight in the far infrared range is of order $\nu_p^2 = 14000^2 \mathrm{cm}^{-2}$, the relative change in spectral weight is of order 0.05 %. Typical accuracy reached for spectral weight estimates using conventional reflection techniques is of order 5%. This illustrates the technical difficulties one has to face when attempting to extract superconductivity induced changes of the kinetic energy.

Experimental limitations on the accuracy are imposed by (i) the impossibility to measure *all* frequencies including the sub-mm range, (ii) systematic errors induced by Kramers-Kronig analysis: The usual procedure is to use data into the visible/ultra-violet range and beyond for completing the Kramers-Kronig analysis in the far infrared, assuming that no important temperature dependence is present outside the far infrared range. Obviously this assumption becomes highly suspicious if the search is concentrated on spectral weight transfer originating from precisely this frequency range.

The remedy is, to let nature perform the spectral weight integral. Due to causality $\mathrm{Re}\epsilon(\omega)$ and $\mathrm{Re}\sigma(\omega)$ satisfy the Kramers-Kronig relation

$$\mathrm{Re}\epsilon(\omega) = 1 - \int_0^\infty \frac{8\mathrm{Re}\sigma(z)}{\omega^2 - z^2} dz \tag{1.58}$$

The main idea of spectral weight transfer is, that spectral weight is essentially transferred from the inter-band transitions at an energy of

several eV, down to the δ-function in $\sigma(\omega)$ at $\omega = 0$. Indeed various groups have reported a change of optical properties in the visible part of the spectrum when the sample becomes superconducting[96, 97, 98, 99]. If this is the case, we have $x = 0$ for the extra spectral weight in relation 1.58. Together with Eq. 1.56 it follows that changes in kinetic energy can be read directly from $\mathrm{Re}\epsilon(\omega)$ using the relation

$$\delta E_{kin}^{eff}(\omega) = \frac{4\hbar^2\omega^2 V_u}{\pi e^2 a^2}\mathrm{Re}\delta\epsilon(\omega) \tag{1.59}$$

If the spectral weight is transferred to a frequency range ω_0, then the above expression can still be applied for $\omega \gg \omega_0$. If we measure $\mathrm{Re}\epsilon(\omega)$ *directly* using spectroscopic ellipsometry, then indeed nature does the integration of $\sigma(\omega)$ for us at each temperature. This eliminates to a large extent various systematic errors affecting the overall accuracy of the spectral weight sum. It is important to measure the complex dielectric constant for a large range of different frequencies.

The second problem is that already above the superconducting phase transition the optical spectra of these materials have appreciable temperature dependence. What we really like to measure is the spectra of the same material in the superconducting state, and in the 'normal' state, both at the same temperature. Typical magnetic fields required to bring the material in the normal state are impractical, let alone the complications of magneto-optics which then have to be faced. A more practical approach is to measure carefully the temperature dependence over a large temperature range, with small temperature intercepts, and to search for changes which occur at the phase transition.

In Fig. 1.11 the spectral weight from 0 to 10000 cm^{-1} is shown as a function of temperature for the case of Bi2212[99]. Note that this integral corresponds to *minus* the ab-plane kinetic energy. We observe, that in the superconducting state the kinetic energy drops by an amount of about 1 meV per Cu. This is in fact a relatively large effect. This surprising result seems to tell us that in the cuprates the kinetic energy in the superconducting state is *lowered* relative to the normal state. This corresponds to the unconventional scenario depicted in the right-hand panel of Fig.1.5, where the normal state is a non Fermi liquid, whereas the superconducting state follows the behavior of a (more) conventional BCS type wave-function with the usual type of Bogoliubov quasi-particles. The amazing conclusion from this would be, that there is no need for a *lowering* of the interaction energy any more. The condensation energy of optimally doped Bi2212 is about 0.1 meV per Cu atom[76].

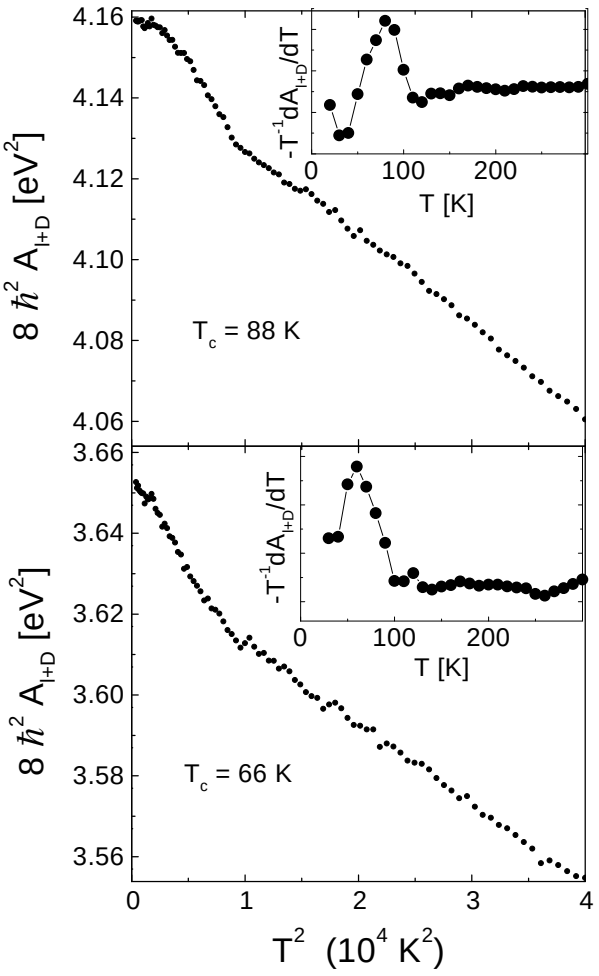

Figure 1.11. Measured values of the quantity $c^2\omega_{p,s}^2 + 8\int_{0^+}^{\infty} \mathrm{Re}\sigma_{ab}(\omega)d\omega$ of Bi2212 (T_c=88 K). The data are taken from Ref. [99, 100]. To make the conversion to kinetic energy summed over the two *ab*-plane directions, the numbers along the vertical axis have to be multiplied with a factor $-10^3 V_u/(4\pi e^2 a^2) = -83$ meV / eV^2.

5. Conclusions

The optical conductivity is a fundamental property of solids, contains contributions of vibrational and electronic character. Among the electronic type of excitations the intra-band and inter-band transitions, exci-

tons, and plasmons of different types correspond to the most prominent features in the spectra. In addition multi-magnon excitations or more exotic collective modes can often be detected. The careful study of the optical properties of solids can provide valuable microscopic information about the electronic structure of solids. In contrast to many other spectroscopic techniques, it is relative easy to obtain reliable absolute values of the optical conductivity. As a result sum rules and sum rule related integral expressions can often be applied to the optical spectra. Here we have treated a few examples of sum rule analysis: Application of the f-sum rule to the phonon spectra of transition metal silicides provides information on the resonant electron-phonon coupling in these materials. Integration of the energy-loss function gives the value of the Coulomb energy stored in the material, which is seen to increase when a high T_c cuprate enters the superconducting state. The spectral weight within the partially band of the high T_c cuprates is seen to become larger in superconducting state. This effect exists both perpendicular to the planes and parallel to the planes. This spectral weight change can be associated with a decrease of kinetic energy when the material becomes superconducting. Although the relative spectral weight change along the ab-plane is quite small, it indicates a fairly large change of the ab-plane kinetic energy, large enough to account for the energy by which the superconducting state of these materials is stabilized. In addition the real and imaginary part of the optical conductivity can be used to study the intrinsic Josephson coupling between the superconducting planes. In superconductors with two or more different types of weak links alternating, such as $SmLa_{1-x}Sr_xCu_4$, $YBa_2Cu_3O_{7-x}$, $Bi_2Sr_2CaCu_2O_8$, a rich spectrum of plasma-oscillations is observed in the superconducting state, and sometimes above T_c, due to the multi-layered structure of these materials. This has provided important insights in the nature of the coupling, and it has been used to extract quantitative values of this coupling.

6. Acknowledgements

Part of the experiments described in this chapter have been carried out by J. H. Kim, J. Schuetzmann, A. Tsvetkov, A. Kuzmenko, G. Rietveld, B. J. Feenstra, H. S. Somal, J. E. van der Eb, A. Damascelli, M. U. Grueninger, D. Dulic, C. Presura, P. Mena, and H. J. A. Molegraaf. The author has benefitted from discussions with, among others, D. I. Khomskii, G. A. Sawatzky, M. J. Rice, P. W. Anderson, A. J. Leggett, Z. X. Shen, S. C. Zhang, A. J. Millis, M. Turlakov, J. E. Hirsch, D. N. Basov, M. R. Norman, and W. Hanke.

References

[1] W. Hanke, and L. J. Sham, Phys. Rev. B **12**, 4501 (1977).

[2] P. Nozières, and D. Pines, Phys. Rev. **111** 442 (1958).

[3] P. Nozières, and D. Pines, Phys. Rev.**113** 1254 (1959).

[4] Note the extra factor of π. In Ref. [2] this factor is absent, but it is recuperated in the final formulas.

[5] The intra-band optical spectrum of a superconductor typically has three contributions: (i) A Dirac-function in the origin corresponding to the supercondensate the presence of which is revealed by a reactive response in the imaginary part of the optical conductivity below the gap diverging as $\sigma_2(\omega) = c^2/(4\pi\lambda(T)^2\omega)$. (ii) A gapped Drude-like peak due absorption of light by pairs of quasi-particles excited above the gap. For $\omega >> 2\Delta$ the spectrum merges with the Drude peak observed in the normal state. (iii) A narrow peak of finite width centered at $\omega = 0$ due to the dissipative response of thermal quasi-particles above the gap.

[6] The proof of Eq. 1.17 follows the same lines as the derivation of the f-sum rule. It employs the fact, that the current operators can be represented as commutators of the hamiltonian with the dipole operator. The expectation value of the hamiltonian is used to cancel out the factor ω_{mn} in the denominator of the expression. In the final step the commutator of the dipole operator and the current operator is calculated in second quantization, which completes the derivation of Eq. 1.17. For a Galilean invariant system at $T = 0$ this summation cannot be carried out directly for $q = 0$. The singular behaviour at this point can be circumvented by considering the limit $q \to 0$.

[7] A. Damascelli, K. Schulte, D. van der Marel, and A.A. Menovsky, Phys. Rev. B **55**, R4863 (1997).

[8] A. Damascelli, Ph D. Thesis, University of Groningen (1999).

[9] M. J. Rice, N. O. Lipari, and S. Strässler Phys. Rev. Lett. **39**, 1359 (1977).

[10] W. A. Challener and P. L. Richards, Solid State Commun. **52**, 117 (1984).

[11] G.Travaglini and P.Wachter, Phys. Rev. B **30**, 1971 (1984).

[12] L. Degiorgi, P. Wachter and C.Schlenker, Phys. Rev. B **164**, 305 (1990).

[13] L. Degiorgi and G. Grüner, Phys. Rev. B **44**, 7820 (1991).

[14] V. Vescoli, L. Degiorgi, B. Buschinger, W. Guth, C. Geibel, and F. Steglich, Solid State Commun. **105**, 367 (1998).

[15] G. Lucovsky, and R. M. White, Phys. Rev. B **8**, 660 (1973).

[16] C. Presura, M.Popinciuc, P. H. M. van Loosdrecht, D. van der Marel, M. Mostovoy, G. Maris, T. T. M. Palstra, H. Yamada, Y. Ueda, Phys. Rev. Lett., in press (2003).

[17] This expression was originally obtained by R. Kubo, J. Phys. Soc. Japan **12**, 570 (1957). Recently it has been used by M. R. Norman, and C. Pepin, Phys. Rev. B **66**, 100506(R) (2002), to analyze the superconductivity induced transfer of spectral weight of high T_c superconductors. See also Eq. 13 of Ref. [24]. The derivation of this expression proceeds along similar lines as the proof of the f-sum rule, see also the comments in Ref. [6]. Due to the non-parabolic energy-momentum dispersion in this case, the commutator of the dipole operator with the current operator produces an inverse *dynamical* mass of the band-electrons which depends on the canonical momentum, instead of a momentum-independent mass.

[18] Pierre F. Maldague, Phys. Rev. **16**, 2437 (1977).

[19] D. Baeriswyl, J. Carmelo, and A. Luther, Phys. Rev. B **33**, 7247 (1986).

[20] D. N. Basov, S. I. Woods, A. S. Katz, E. J. Singley, R. C. Dynes, M. Xu, D. G. Hinks, C. C. Homes, M. Strongin, Science **283**, 49 (1999).

[21] S. Chakravarty, H. Kee, E. Abrahams, Phys. Rev. Lett. **82**, 2366 (1999).

[22] S. Spielman, B. Parks, J. Orenstein, D. T. Nemeth, F. Ludwig, J. Clarke, P. Merchant, and D. J. Lew, Phys. Rev. Lett. **73**, 1537 (1994).

[23] S. G. Kaplan, S. Wu, H. T. S. Lihn, D. Drew, Q. Li, D. B. Fenner, Julia Phillips, and S. Y. Hou, Phys. Rev. Lett. **76**, 696 (1996).

[24] H. D. Drew, and P. Coleman, Phys. Rev. Lett., Vol. **78**, 1572 (1997).

[25] G. Mahan 'Many-Particle Physics', Plenum press (New York, 1981).

[26] P. Nozières and D. Pines, 'The theory of quantum liquids' part I, W. A. Benjamin 1966.

[27] Misha Turlakov, Anthony J. Leggett, cond-mat/0207422.

[28] D. N. Basov, E. J. Singley, S. V. Dordevic, Phys. Rev. B **65**, 054516 (2002).

[29] N. Shah, A. J. Millis, Phys. Rev. B **64**, 174506 (2001).

[30] A. Abanov, A. V. Chubukov, Phys. Rev. Lett. **88**, 217001 (2002).

[31] D. van der Marel, Physica C **165**, 35 (1990).

[32] D. van der Marel, and G. Rietveld, Phys. Rev. Lett. **69**, 2575 (1992).

[33] G. Rietveld, N. Y. Chen, D. van der Marel, Phys. Rev. Lett. **69**, 2578 (1992).

[34] D. van der Marel, D. I. Khomskii and G.M. Eliashberg, Phys. Rev. B **50**, 16594 (1994).

[35] A. J. Leggett, Proc. Natl. Acad. Sci. USA Vol. **96**, 8365 (1999).

[36] C. N. Presura, Ph D. Thesis, University of Groningen (2003).

[37] M. R. Norman, M. Randeria, B. Janko, J. C. Campuzano, Phys. Rev. B **61**, 14724 (2000).

[38] R. Micnas, J. Ranninger, and S. Robaszkiewicz, Rev. Mod. Phys. **62**, 113 (1990).

[39] P. Nozières, and S. Schmitt-Rink, J. Low Temp. Phys **59**, 195 (1985).

[40] D. van der Marel, Phys. Rev. B. **51**, 1147 (1995).

[41] P. W. Anderson, Science **268**, 1154 (1995).

[42] S. Chakravarty, Eur. Phys. J. B **5**, 337 (1998).

[43] J. E. Hirsch, Physica C **199**, 305 (1992).

[44] J. E. Hirsch, Physica C **201**, 347 (1992).

[45] S. Chakravarty, A. Sudbo, P. W. Anderson, and S. Strong, Science **261**, 337 (1993).

[46] S. Alexandrov and N. F. Mott, High Temperature Superconductors and Other Superfluids (Taylor and Francis, 1994).

[47] V. Emery and S. A. Kivelson, Nature **374**, 4347 (1995).

[48] F. F. Assaad, M. Imada, and D. J. Scalapino, Phys. Rev. Lett. **77**, 4592 (1996).

[49] P. A. Lee, Physica C **317**, 194 (1999).

[50] P. W. Anderson, Physica C **341-348**, 9 (2000).

[51] V. J. Emery, S. A. Kivelson, J. Phys. Chem. Solids **61**, 467 (2000).

[52] A. J. Leggett, Science **274**, 587 (1996).

[53] D. van der Marel, H.S. Somal, B.J. Feenstra, J.E. van der Eb, J. Schuetzmann, Jae Hoon Kim. Proc. 10th Ann. HTS Workshop on Physics, Houston, World Sc. Publ., page 357 (1996).

[54] J. Schuetzmann, H.S. Somal, A.A. Tsvetkov, D. van der Marel, G. Koops, N. Koleshnikov, Z.F. Ren, J.H. Wang, E. Brueck and A.A. Menovski, Phys. Rev. B **55**, 11118 (1997).

[55] C. Panagopoulos, J. R. Cooper, T. Xiang, G. B. Peacock, I. Gameson, and P. P. Edwards, Phys. Rev. Lett. **79**, 2320 (1997) .

[56] A. Tsvetkov, D. van der Marel, K. A. Morel, J. R. Kirtley, J. L. de Boer, A. Meetsma, Z. F. Ren, N. Koleshnikov, D. Dulic, A. Damascelli, M. Grüninger, J. Schützmann, J. W. van der Eb, H. S. Somal, and J. H. Wang, Nature **395**, 360 (1998).

[57] K. A. Moler, J. R. Kirtley, D. G. Hinks, T. W. Li, and Ming Xu, Science **279**, 1193 (1998).

[58] J. R. Kirtley, K.A. Moler, G. Villard, A. Maignan, Phys. Rev. Lett. **81**, 2140 (1998).

[59] M.B. Gaifullin, Yuji Matsuda, N. Chikumoto, J. Shimoyama, K. Kishio, and R. Yoshizaki, Phys. Rev. Lett. **83**, 3928 (1999).

[60] D. N. Basov, C. C. Homes, E. J. Singley, M. Strongin, T. Timusk, G. Blumberg, and D. van der Marel, Phys. Rev. B **63**, 134514 (2001).

[61] V. Zelezny, S. Tajima, D. Munzar, T. Motohashi, J. Shimoyama, and K. Kishio, Phys. Rev. B **63**, 060502 (2001).

[62] Dominik Munzar, Christian Bernhard, Todd Holden, Andrzej Golnik, Josef Humlicek, and Manuel Cardona, Phys. Rev. B **64**, 024523 (2001).

[63] Dominik Munzar, Todd Holden, Christian Bernhard, Phys. Rev. B **67**, R020501 (2003).

[64] A.V Boris, D. Munzar, N.N. Kovaleva, B. Liang, C.T. Lin, A. Dubroka, A.V. Pimenov, T. Holden, B. Keimer, Y. -L. Mathis, C. Bernhard, Phys. Rev. Lett. **89**, 277001 (2002).

[65] S. L. Cooper, and K.E. Gray, *Physical Properties of High Temperature Superconductors IV*, ed. D. M. Ginsberg (World Scientific, Singapore 1994).

[66] Jae H. Kim, H.S. Somal, D. van der Marel, A.M. Gerrits, A. Wittlin, V.H.M. Duijn, N.T. Hien and A.A. Menovsky, Physica C **247**, 297 (1995).

[67] D. Dulic, D. van der Marel, A. A. Tsvetkov, W. N. Hardy, Z. F. Ren, J. H. Wang, B. A. Willemsen, Phys. Rev. B **60**, R15051 (1999).

[68] A. Hosseini, S. Kamal, D.A. Bonn, Ruixing Liang, and W.N. Hardy, Phys. Rev. Lett. **81**, 1298 (1998).

[69] K. Tamasaku, Y. Nakamura, and S. Uchida, Phys. Rev. Lett. **69**, 1455 (1992).

[70] J. W. Loram,K. A. Mirza, J. M. Wade, J. R. Cooper, and W. Y. Liang, Physica C **235-240**, 134 (1994).

[71] D. van der Marel, A.J. Leggett, J.W. Loram, J.R. Kirtley Phys. Rev. B **66**, 140501R (2002).

[72] M. Tinkham, and R. A. Ferrell, Phys. Rev. Lett. **2**, 331 (1959).

[73] D. Munzar, C. Bernhard, A. Golnik, J. Humlicek, M. Cardona, Solid State Commun. **112**, 365 (1999).

[74] V. Zelezny, S. Tajima, T. Motohashi, J. Shimoyama, K. Kishio, and D. van der Marel, J. Low Temp. Phys. **117**, 1019 (1999).

[75] M. Grueninger, D. van der Marel, A.A. Tsvetkov, A. Erb, Phys. Rev. Lett. **84**, 1575 (2000).

[76] J. W. Loram, J. Luo, J. R. Cooper, W. Y. Liang and J. L. Tallon, J. Phys. Chem. Solids **62**, 59 (2001).

[77] D. van der Marel, A. Tsvetkov, Czech. J. Phys. **46**, 3165 (1996).

[78] D. van der Marel, and A. A. Tsvetkov, Phys. Rev. B **64**, 024530 (2001).

[79] N. Shah, A. J. Millis, Phys. Rev. B **65**, 024506 (2002).

[80] H. Shibata and T. Yamada, Phys. Rev. Lett. **81**, 3519 (1998).

[81] H. Shibata, Phys. Rev. Lett. **86**, 2122 (2001).

[82] T. Kakeshita, S. Uchida, K. M. Kojima, S. Adachi, S. Tajima, B. Gorshunov und M. Dressel, Phys, Rev. Lett. **86**, 4140 (2001).

[83] D. Dulic, A. Pimenov, D. van der Marel, D.M. Broun, S. Kamal, W.N. Hardy, A.A. Tsvetkov, I.M. Sutjaha, Ruixing Liang, A.A. Menovsky, A. Loidl and S.S. Saxena, Phys. Rev. Lett. **86**, 4144 (2001).

[84] A. Pimenov, A. Loidl, D. Dulic, D. van der Marel, and A. A. Menovsky, Phys. Rev. Lett. **87**, 177003 (2001).

[85] D. Dulic, Ph D. Thesis, University of Groningen (2000).

[86] M. Grueninger, Ph D. Thesis, University of Groningen (1999).

[87] J. E. Hirsch, and F. Marsiglio, Physica C **331**, 150 (1999).

[88] J. Bonca, P. Prelovsek, and I. Sega, Phys. Rev. B **39**, 7074 (1989).

[89] J. A. Riera, Phys. Rev. B **40**, 833 (1989).

[90] Y. Hasegawa, and D. Poilblanc, Phys. Rev. B **40**, 9035 (1989).

[91] E. Dagotto, J. Riera, and A.P. Young, Phys. Rev. B **42**, 2347 (1990).

[92] T. Barnes, A. E. Jacobs, M. D. Kovarik, and W. G. Macready, Phys. Rev.B **45**, 256 (1992).

[93] E. Demler, and S.-C. Zhang, Nature **396**, 733 (1998).

[94] I. Fugol, V. Samovarov, A. Ratner, V. Zhuravlev, G. Saemann-Ischenko, B. Holzapfel, and O. Meyer, Solid State Commun. **86**, 385 (1993).

[95] Y. Yagil, E. K. H. Salje, Physica C **256**, 205 (1996).

[96] M. J. Holcomb, J. P. Collman, and W. A. Little, Phys. Rev. Lett. **73**, 2360 (1994).

[97] W. A. Little, K. Collins, and M. J. Holcomb, J. Superconductivity **12**, 89 (1999).

[98] M. Rübhausen, A. Gozar, M. V. Klein, P. Guptasarma, D. G. Hinks, Phys. Rev. B **63**, 224514 (2001).

[99] H. J. A. Molegraaf, C. Presura, D. van der Marel, P. H. Kes , M. Li, Science **295**, 2239 (2002). Similar conclusions have been obtained in Ref. [100].

[100] A.F. Santander-Syro, R.P.S.M. Lobo, N. Bontemps, Z. Konstantinovic, Z.Z. Li, H. Raffy, cond-mat/0111539.